Energy-Efficient Multi-Access Mobile Edge Computing With Secrecy Provisioning

Li Ping Qian, *Senior Member, IEEE*, Yuan Wu, *Senior Member, IEEE*, Ningning Yu, Daohang Wang, Fuli Jiang, and Weijia Jia, *Fellow, IEEE*

Abstract—Thanks to the wide deployment of heterogeneous radio access networks (RANs) in the past decades, the emerging paradigm of multi-access mobile edge computing, which allows mobile terminals to simultaneously offload the computation-workloads to several different edge-computing servers via multi-RANs, has provided a promising scheme for enabling the computation-intensive mobile Internet services in future wireless systems. The broadcasting nature of radio transmission, however, may lead to a potential secrecy-outage during the offloading transmission. In this paper, we thus investigate the energy-efficient multi-access mobile edge computing with secrecy provisioning. Specifically, we first investigate the scenario of one wireless device's (WD's) multi-access offloading subject to a malicious node's eavesdropping. By characterizing the WD's secrecy based throughput in its offloading transmission, we formulate a joint optimization of the WD's multi-access computation offloading, secrecy provisioning, and offloading-transmission duration, with the objective of minimizing the WD's total energy consumption, while providing a guaranteed secrecy-outage during offloading and a guaranteed overall-latency in completing the WD's workload. Despite the non-convexity of this joint optimization problem, we exploit its layered structure and propose an efficient algorithm for solving it. Based on the study on the single-WD scenario, we further investigate the scenario of multiple WDs, in which a group of WDs sequentially execute the multi-access computation offloading, while subject to a malicious node's eavesdropping. Taking the coupling effect among different WDs into account, we propose a swapping-heuristic based algorithm (that uses our proposed single-WD algorithm as a subroutine) for finding the ordering of the WDs to execute the multi-access computation offloading, with the objective of minimizing all WDs' total energy consumption. Extensive numerical results are provided to validate the effectiveness and efficiency of our proposed algorithms. The results demonstrate that our algorithms can outperform some conventional fixed offloading scheduling scheme and randomized offloading ordering scheme.

Index Terms—Multi-access mobile edge computing, secrecy-driven computation offloading, and joint computation and communication resource allocations

1 Introduction

Driven by the rapid development of fifth generation (5G) cellular networks and services, the past decade has witnessed an explosive growth of emerging mobile Internet services and Internet of Things applications such as unmanned vehicles, robotics, and virtual/mixed reality, which are computation-intensive yet delay-sensitive. However, the limited computation-units of conventional wireless devices (e.g., due to the issues of cost and size) lead to a heavy pressure on running these computation-intensive services and a degraded quality of experience consequently. Mobile edge computing (MEC), which deploys a sufficient amount of computation-resources at the edge of wireless networks (e.g., macro/micro base stations or access points) and allows wireless devices to offload parts of computation tasks to nearby edge-computing servers, has provided a promising paradigm to address this issue [1], [2]. Compared to traditional cloud computing, MEC avoids sending the tasks to central cloud servers via Internet, which thus efficiently reduces the latency in completing the tasks as well as saves the transmission bandwidth for sending the tasks. Thanks to its great potentials, the paradigm of MEC has attracted lots of research efforts in the past years [3].

In particular, due to invoking radio transmission between the wireless devices and edge-computing servers, MEC necessitates a proper coordination between the computation offloading and resource allocation [4]. Such a coordinated management is expected to play an even more crucial role in the emerging paradigm of multi-access MEC [5], [6]. In recent years, the emerging paradigm of multi-access MEC (or multi-access computation offloading) has attracted growing attentions. Different from the

- *Li Ping Qian, Ningning Yu, and Daohang Wang are with the College of Information Engineering, Zhejiang University of Technology, Hangzhou 310023, China. E-mail: lpqian@zjut.edu.cn, {nnyu_zjut, dhwang_zjut}@163.com.*
- *Yuan Wu is with the State Key Laboratory of Internet of Things for Smart City, University of Macau, Macao, China. E-mail: yuanwu@um.edu.mo.*
- *Yuan Wu is with the Department of Computer and Information Science, University of Macau, Macao, China, and also with the Zhuhai-UM Science and Technology Research Institute, Zhuhai, China. E-mail: yuanwu@um.edu.mo.*
- *Fuli Jiang is with the State Key Laboratory of Internet of Things for Smart City, University of Macau, Macao, China. E-mail: fljiangcisum@gmail.com.*
- *Weijia Jia is with the BNU-UIC Institute of Artificial Intelligence and Future Networks, Beijing Normal University (BNU Zhuhai), Zhuhai 519085, China, and also with the Guangdong Key Lab of AI and Multi-Modal Data Processing, BNU-HKBU United International College, Zhuhai, Guangdong 519085, China. E-mail: jiawj@uic.edu.cn.*

Manuscript received 21 Sept. 2020; revised 4 Feb. 2021; accepted 17 Mar. 2021. Date of publication 25 Mar. 2021; date of current version 5 Dec. 2022. (Corresponding author: Yuan Wu.)
Digital Object Identifier no. 10.1109/TMC.2021.3068902

conventional paradigm of computation offloading in which an user can only be associated with one edge-computing server, the paradigm of multi-access computation offloading allows an user to offload its computation-workloads to several servers simultaneously (e.g., via the recent advanced multi-homing radio access). Specifically, the user can divide its computation-workload into several pieces and offload these pieces to different servers. Such a multi-access feature not only enables a flexible exploitation of the computation-resources provided by different edge servers, but also provides a great freedom in user's offloading scheduling. Therefore, the multi-access computation offloading has been expected to effectively improve the efficiency in computation offloading, e.g., reducing the total energy consumption. As a result, taking the multi-access feature into account, it is of a crucial importance to investigate the joint multi-access computation offloading and communication-resource allocation for achieving the benefits of multi-access MEC.

Meanwhile, the security issues of MEC have also attracted lots of attentions in recent years. In particular, due to the broadcasting nature of radio transmission, one of the crucial security issues in multi-access MEC is that the offloaded tasks from the wireless devices might be eavesdropped by a malicious node. For instance, a malicious node may intentionally collect the radio signal from a wireless device which is offloading tasks and decode the task data in a brute-force manner. Therefore, aggressively offloading computation-workload but without a secrecy provisioning may result in a significant amount of computation-workloads eavesdropped. It has been a critical question about how to exploit the feature of multi-access computation offloading for improving the offloading performance of a wireless device (e.g., its energy consumption in completing the tasks), while providing a guaranteed secrecy for offloading transmission as well as a guaranteed latency in completing the task. Such a solution strongly depends on a proper management of the computation offloading, secrecy provisioning, and offloading transmission. Furthermore, this question will become even more challenging if we consider the scenario of multiple wireless devices. Due to sharing the computation resources at the edge-computing servers, the latency of different wireless devices are inherently coupled, which further necessitates a proper ordering of different wireless devices for executing computation offloading. Motivated by the above considerations, in this work, we investigate the energy efficient multi-access MEC with secrecy provisioning. Our contributions can be summarized as follows.

- *(Single-WD scenario):* We first focus on the scenario of one WD's multi-access offloading subject to a malicious node's eavesdropping-attack. We adopt the metric of physical layer security [33], [34] and drive the WD's secrecy based offloading throughput by analyzing its secrecy-outage probability. Furthermore, we formulate a joint optimization of the WD's multi-access computation offloading, secrecy provisioning, and offloading-transmission duration, with the objective of minimizing the WD's total energy consumption in completing the required workload, while providing a guaranteed secrecy-outage requirement and a guaranteed latency requirement in completing the workload. Despite the non-convexity of the formulated joint optimization problem, we identify the hidden convexity under the given secrecy-provisioning and transmission-duration, and analytically characterize the consequently optimal WD's multi-access offloading decision. Exploiting this feature, we propose an efficient layered algorithm for solving the joint optimization problem.
- *(Multi-WD scenario):* Based on our proposed algorithm for the single-WD scenario, we further investigate the scenario of multiple WDs, in which a group of WDs sequentially execute the multi-access computation offloading, while subject to a malicious node's eavesdropping. Due to sharing the computation-resources at different edge-computing servers in a time-division manner, the overall-latency of different WDs for completing their respective workloads are coupled and depend on the ordering of the WDs for executing multi-access offloading. Therefore, exploiting our proposed single-WD algorithm as a subroutine, we first propose an myopic algorithm for obtaining the total energy consumption of all WDs under a given offloading ordering. Next, we propose a swapping-heuristic based algorithm for finding the ordering of the WDs in executing multi-access computation offloading, with the objective of minimizing all WDs' total energy consumption.

The remainder of this work is organized as follows. Section 2 reviews the related studies. We present the system model and problem formulation in Section 3. Section 4 presents our proposed algorithm for solving the single-WD scenario. We further investigate the multi-WDs scenario in Section 5 and illustrate the algorithm design in Section 6. Section 7 finally concludes this work and discusses the future direction.

2 Literature Review

Many research efforts have been devoted to investigating the computation offloading for reaping the benefits of multi-access MEC. In [7], Guo *et al.* proposed a greedy computation offloading scheme for multi-access MEC in ultra-dense networks. An incentive based task offloading scheme has been proposed for multi-access MEC in [8]. In [9], a dynamic scheme for task offloading and scheduling has been proposed for low-latency services in multi-access MEC. In [10], Chen *et al.* exploited the deep reinforcement learning for optimizing computation offloading performance. Optimal workload allocation scheme for balancing the delay and power consumption has been studied in [11]. In [12], Pham *et al.* investigated the computation offloading problem in multi-carrier non-orthogonal multiple access enabled MEC systems and adopted the coalition formation game to solve the problem. Taking the intermittent connectivity into account, Zhang *et al.* proposed a dynamic computation offloading scheme for minimizing the computation and offloading costs [13]. In [14], Liu *et al.* proposed a multiple-objective optimization that accounts for the energy consumption, execution delay, and payment cost in

computation offloading. A learning-based offloading mechanism has been proposed for a scenario of multi-user and multi-edge-node [15]. In [16], Zhang *et al.* proposed an incentive-mechanism based computation offloading for blockchain systems.

In particular, the joint optimization of the computation offloading and resource allocation is crucial to achieve the advantages of multi-access MEC. In [17], a joint optimization scheme for offloading scheduling and power allocation has been proposed for MEC systems. In [18], a joint optimization of computation offloading and offloading-transmission has been proposed for users' multi-access offloading for minimizing the latency in completing tasks. A joint task offloading and resource allocation scheme that accounts for the channel dynamics has been proposed in [19]. In [20], Sheng *et al.* exploited the users' differentiated uploading delay and proposed a joint offloading decision and resource allocation scheme for reducing the users' average offloading delay. A dynamic resource management scheme has been proposed for multi-access MEC in autonomous vehicular network in [21]. In [22], Gu *et al.* proposed a joint radio and computational resource allocation based on the matching game framework. A joint optimization of radio and computational resources allocation has been proposed for blockchain-enabled MEC system in [23].

In addition to latency minimization, there have been many studies investigating the energy-efficiency of MEC. In [24], the authors adopted the consensus alternating direction method of multipliers (ADMM) approach for optimizing the energy-efficiency in edge computing. In [25], Chang *et al.* developed the queuing model to investigate the multi-user energy-efficient computation offloading problem. In [26], a joint optimization of resource allocation and trajectory has been developed for energy-efficient unmanned aerial vehicle (UAV) assisted MEC. In [27], Haber *et al.* proposed a joint optimization of computational cost and energy consumption for task offloading in multi-tier edge-cloud systems. In [28], an energy-efficient offloading scheme has been proposed for the multi-task multi-access computation offloading. In [29], Zhang *et al.* incorporated the multi-access characteristics of the 5G heterogeneous network and designed an energy-efficient computation offloading scheme which jointly optimizes offloading and radio resource allocation to minimize the energy consumption under the latency constraints. In addition to the aforementioned studies focusing on optimizing the energy consumption, wireless power transfer and energy harvesting have also been exploited for improving the energy-efficiency of MEC [30], [31], [32]. In [30], Min *et al.* proposed a reinforcement learning based computation offloading scheme for Internet of Things (IoT) devices with energy harvesting. In [31], a computation-rate maximization scheme has been proposed for wireless powered MEC with binary computation offloading. However, the aforementioned studies do not account for the security issue (i.e., the eavesdropping-attack) in the offloading transmission, and thus cannot provide a guaranteed secrecy-provisioning for edge-computing users. Different from the above studies, we aim at providing a guaranteed secrecy-provisioning to encounter the eavesdropping-attack during the user's offloading transmission, and propose a joint optimization of the secrecy-provisioning, the user's offloading transmission and its multi-access offloading decision to study this problem.

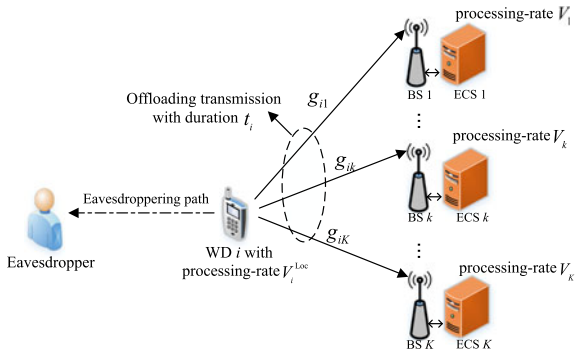

Fig. 1. Illustrative system model of one WD's multi-access offloading subject to the eavesdropping-attack.

The growing concerns on security issue in MEC have motivated lots of research interests in recent years. In particular, the physical layer security [33], [34], stemming from the classic information theory, provides a fundamental measure of secure throughput which cannot be overheard by any eavesdropper. Thanks to the advantages, the physical layer security and the associated secrecy-outage probability have been widely exploited for securing different paradigms of wireless networks [35], [36], [37], [38], [39]. Several recent studies have investigated secure mobile edge computing by exploiting physical layer security. In [40], Xu *et al.* exploited physical layer security to secure the multiuser computation offloading from being overheard by the eavesdropper. In [41], a secrecy driven resource management scheme has been proposed for vehicular computation offloading. In [42], Wu *et al.* exploited non-orthogonal multiple access (NOMA) for multi-user computation offloading and investigated the weighted sum-energy consumption minimization problem subject to the secrecy offloading rate constraints. However, the feature of multi-access computation offloading has not been taken into account in the aforementioned studies [40], [41], [42], which thus necessitates us to investigate the joint optimization of the multi-access offloading and the secrecy provisioning. To this end, it is of a crucial importance to characterize the connections between the WD's offloading transmission, secrecy-provisioning, and the multi-access offloading decisions, which however are seldom discussed in the existing studies before.

3 Problem Formulation for Single-WD Scenario

We first study the single-WD scenario as shown in Fig. 1, in which one WD (denoted by WD i) executes multi-access computation offloading to a group of edge-computing servers (ECSs) subject to the eavesdropping-attack of a malicious node. Specifically, WD i is running a task with the computation-workload requirement S_i^{req} and the latency-requirement $T_i^{\max}$. Meanwhile, there exist a group of K ECSs denoted by $\mathcal{K} = \{1, 2, \ldots, K\}$, which can accommodate the offloaded computation-workloads from WD i. We use vector $\mathbf{s}_i = (s_{i1}, s_{i2}, \ldots, s_{iK})$ to denote WD i's offloaded workloads to different ECSs, with s_{ik} denoting the workload offloaded to ECS k. In this work, we consider that WD i uses

frequency division multiple access (FDMA) to send $\mathbf{s}_i$ to the ECSs simultaneously. Due to the open access nature of radio transmission, a malicious node can intentionally overhear WD i's offloaded data by collecting the radio signal from WD i and further decode the signals (e.g., in a brute-force manner). We will next quantify how secure it is when WD i offloads its task to ECS k in the next subsection.

We emphasize that in this work, we first investigate the single-WD multi-access offloading subject to the eavesdropping-attack in Sections 3 and 4, which provides an important basis for us to further investigate a more complicated scenario of multi-WDs' multi-access offloading in Sections 5 and 6. As we will illustrate soon, even the study on the single-WD multi-access offloading is challenging, since it invokes a complicated non-convex joint optimization problem of the multi-access offloading, secrecy provisioning, and offloading transmission. To focus on our design of multi-access computation offloading under the eavesdropping-attack, we mainly consider a relatively static scenario, in which the channel power gains from the WD to different ECSs are known and keep unchanged within a duration of interests. Nevertheless, the eavesdropper may intentionally hide its location, which results in that the channel power gain from the WD to the eavesdropper cannot be obtained. To account for this uncertainty, we adopt the measure of secrecy-outage probability and derive an effectively secure throughput for the WD's offloading-transmission to each ECS, which thus facilitates our problem formulation of multi-access computation offloading with secrecy-provisioning. We will present the details in the next subsection.

3.1 Modeling of Secrecy Driven Computation Offloading

As shown in Fig. 1, when WD i sends its offloaded workload s_{ik} to ECS k, the malicious eavesdropper may overhear the offloaded data. According to the principle of physical layer security [33], the secure throughput from WD i to ECS k can be expressed as

$$C_{ik}^{\mathrm{sec}} = \left(W_k \log_2\left(1+\frac{p_{ik}g_{ik}}{n_k}\right) - W_k \log_2\left(1+\frac{p_{ik}g_{ik\mathrm{E}}}{n_{k\mathrm{E}}}\right)\right)^+.$$

Here, function $(x)^+$ means $\max\{x, 0\}$. p_{ik} denotes WD i's transmit-power to ECS k. Parameter W_k denotes the channel bandwidth of ECS k, g_{ik} denotes the channel power gain from WD i to ECS k, and $g_{ik\mathrm{E}}$ denotes the channel power gain from WD i to eavesdropper on ECS k's channel. Parameter n_k denotes the powers of the background noise at ECS k, and $n_{k\mathrm{E}}$ denotes the power of the background noise at the eavesdropper on ECS k's channel.

However, the value of $g_{ik\mathrm{E}}$ cannot be accurately obtained, since the eavesdropper may intentionally hide its location. Thus, we adopt the measure of secrecy-outage probability [34], [35] and assume that $g_{ik\mathrm{E}}$ follows the exponential distribution with the mean equal to $\alpha_{i\mathrm{E}}$ (notice that $\alpha_{i\mathrm{E}}$ denotes the average eavesdropping-path strength). Mathematically, we can express WD i's secrecy-outage probability P_{ik}^{out} when offloading to ECS k as a function of its transmit-power p_{ik} and the assigned offloading-rate x_{ik} as

$$P_{ik}^{\mathrm{out}}(p_{ik}, x_{ik}) = \Pr\left\{x_{ik} \geq C_{ik}^{\mathrm{sec}} | \log_2\left(1+\frac{p_{ik}g_{ik}}{n_k}\right) \geq \log_2\left(1+\frac{p_{ik}g_{ik\mathrm{E}}}{n_{k\mathrm{E}}}\right)\right\}.$$

Let us further introduce variable ϵ_i to denote the secrecy-outage probability when WD i is offloading to ECS k. By setting $\epsilon_i = P_{ik}^{\mathrm{out}}(p_{ik}, x_{ik})$, we can obtain the following result:

$$x_{ik} = W_k \log_2\left(\frac{p_{ik}\hat{g}_{ik} + n_{k\mathrm{E}}}{p_{ik}\theta_{ik} + n_{k\mathrm{E}}}\right), \tag{1}$$

where parameter $\hat{g}_{ik} = \frac{n_{k\mathrm{E}}}{n_k} g_{ik}$, and the auxiliary parameter θ_{ik} is given by:

$$\theta_{ik} = -\alpha_{i\mathrm{E}} \ln\left(1 - \left(1 - e^{-\frac{\hat{g}_{ik}}{\alpha_{i\mathrm{E}}}}\right)(1-\epsilon_i)\right). \tag{2}$$

Notice that the offloading-rate x_{ik} given in (1) represents WD i's *effectively secure throughput* to ECS k with the specified secrecy-outage probability ϵ_i. In particular, the auxiliary parameter θ_{ik} in (2) captures both the impacts from ϵ_i (i.e., the secrecy-outage probability) and $\alpha_{i\mathrm{E}}$ (i.e., the average strength of eavesdropping-path). It can be verified that θ_{ik} decreases when ϵ_i increases (i.e., a weaker secrecy-provisioning), which yields an increase in x_{ik} according to (1). Meanwhile, θ_{ik} increases when $\alpha_{i\mathrm{E}}$ increases (i.e., a stronger eavesdropping-path), which yields a decrease in x_{ik}. Both the aforementioned two trends are consistent with the intuitions.

With x_{ik} in (1), WD i's offloaded workload s_{ik}, and transmission-duration t_i, we can derive

$$s_{ik} = x_{ik}(1-\epsilon_i)t_i \Leftrightarrow x_{ik} = \frac{s_{ik}}{(1-\epsilon_i)t_i}. \tag{3}$$

Thus, by exploiting (1) and (3), we can express WD i's required transmit-power p_{ik} for its offloading-transmission to ECS k as

$$p_{ik} = \frac{n_{k\mathrm{E}} 2^{\frac{s_{ik}}{t_i W_k (1-\epsilon_i)}} - n_{k\mathrm{E}}}{\hat{g}_{ik} - \theta_{ik} 2^{\frac{s_{ik}}{t_i W_k (1-\epsilon_i)}}}, \tag{4}$$

which depends on WD i's offloaded workload s_{ik} to ECS k, transmission-duration t_i, and the specified secrecy-outage probability ϵ_i. Notice that (4) will be used in our following problem formulation.

In particular, a keen observation on Eq. (1) is that $x_{ik} \leq W_k \log_2\left(\frac{\hat{g}_{ik}}{\theta_{ik}}\right)$, which thus leads to the following constraint on WD i's offloaded workload to ECS k due to Eq. (3):

$$s_{ik} \leq (1-\epsilon_i) t_i W_k \log_2\left(\frac{\hat{g}_{ik}}{\theta_{ik}}\right). \tag{5}$$

3.2 Problem Formulation for Single-WD Scenario

We use V_k to denote the computing-rate provided by ECS k, and V_i^{loc} to denote WD i's local computing-rate. Thus, the overall latency for WD i to complete its total workload S_i^{req} can be given by:

$$L_i = \max\left\{t_i + \max_{k\in\mathcal{K}}\{\frac{s_{ik}}{V_k}\}, \frac{S_i^{\mathrm{req}} - \sum_{k\in\mathcal{K}} s_{ik}}{V_i^{\mathrm{Loc}}}\right\}, \tag{6}$$

where $t_i + \frac{s_{ik}}{V_k}$ denotes the latency for WD i's computation offloading via ECS k, and thus $t_i + \max_{k\in\mathcal{K}}\{\frac{s_{ik}}{V_k}\}$ denotes the latency when WD i offloads $\{s_{ik}\}_{k\in\mathcal{K}}$ to the respective ECSs in parallel via multi-access offloading. Meanwhile, $\frac{S_i^{\mathrm{req}}-\sum_{k\in\mathcal{K}} s_{ik}}{V_i^{\mathrm{Loc}}}$ denotes the latency for WD i to complete its remaining workloads which are not offloaded to the ECSs. As a result, the overall latency for WD i to complete its total workload can be given in Eq. (6) above. In this work, similar to [17], [18], [19], [20], we assume that the latency for the ECSs to send the computation-results back to WD i is negligible, and thus is not included in Eq. (6).

Based on the above modelings, we formulate a joint optimization of WD i's computation offloading $\mathbf{s}_i$, the secrecy-provisioning ϵ_i, and resource allocation t_i. Our objective is to minimize WD i's total energy consumption as follows ("TECM" means "total energy consumption minimization"):

$$\begin{aligned}
&(\mathrm{TECM}): E_i^{\min} = \min \frac{S_i^{\mathrm{req}} - \sum_{k\in\mathcal{K}} s_{ik}}{V_i^{\mathrm{Loc}}}\rho_i^{\mathrm{Loc}} + t_i \sum_{k\in\mathcal{K}} p_{ik} \\
&\text{subject to: } 0 \le s_{ik} \le S_i^{\mathrm{req}}, \forall k, && (7)\\
&\sum_{k\in\mathcal{K}} s_{ik} \le S_i^{\mathrm{req}}, && (8)\\
&0 \le \epsilon_i \le \epsilon_i^{\max}, && (9)\\
&L_i \le T_i^{\max}, && (10)\\
&\text{constraints } (4), (5), \text{ and } (6),\\
&\text{variables: } \mathbf{s}_i, t_i \text{ and } \epsilon_i.
\end{aligned}$$

In the objective function, the part of $t_i \sum_{k\in\mathcal{K}} p_{ik}$ denotes WD i's energy consumption for transmitting the offloaded workloads $\mathbf{s}_i$ to the ECSs. Meanwhile, the part of $\frac{S_i^{\mathrm{req}}-\sum_{k\in\mathcal{K}} s_{ik}}{V_i^{\mathrm{Loc}}}\rho_i^{\mathrm{Loc}}$ denotes WD i's energy consumption for its local computing, with ρ_i^{Loc} denoting WD i's power-consumption coefficient for the local computing. Constraint (7) means that each WD i's offloaded workload s_{ik} to ECS k cannot exceed S_i^{req}. Constraint (8) means that WD i's total amount of the offloaded workload cannot exceed S_i^{req}. Constraint (9) means that the secrecy-outage probability ϵ_i cannot exceed WD i's secrecy-requirement denoted by $\epsilon_i^{\max}$. Notice that according to (4), the value of ϵ_i influences WD i's required transmit-power in its offloading transmission with the specified secrecy-outage probability ϵ_i. Thus, it is crucial to properly control ϵ_i for minimizing the total energy consumption. Constraint (10) means that WD i's overall latency in completing its task cannot exceed its delay-limit $T_i^{\max}$. Notice that in Problem (TECM), we do not treat p_{ik} as a direct variable to be optimized, since it can be substituted by the decision variables ($\mathbf{s}_i$, ϵ_i, t_i) via (4). It is noticed that Problem (TECM) is always feasible if $\frac{S_i^{\mathrm{req}}}{V_i^{\mathrm{Loc}}} \le T_i^{\max}$ holds, meaning that WD i can complete its total computation-workload locally (without invoking any offloading) within its latency-limit.

Problem (TECM), however, is a strictly non-convex optimization, which is challenging to solve. Our key to solve Problem (TECM) lies in that we identify a feature of convexity under the given tuple of (t_i, ϵ_i), with which we can analytically characterize WD i's optimal multi-access offloading decision correspondingly. Motivated by this, we adopt a vertical decomposition of Problem (TECM) into a top-problem for optimizing (t_i, ϵ_i) and a consequent subproblem for optimizing $\mathbf{s}_i$ (under the given tuple of (t_i, ϵ_i)), and propose a corresponding layered-algorithm for solving Problem (TECM) efficiently. The details are shown in the next subsection.

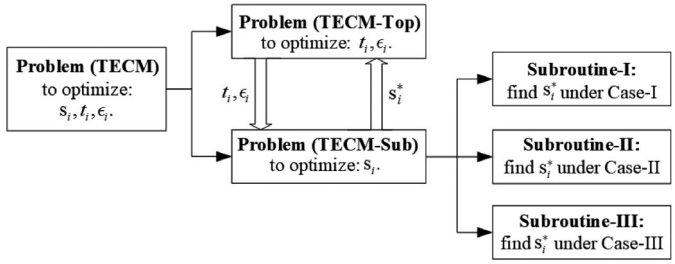

Fig. 2. A vertical decomposition of problem (TECM).

3.3 Layer Structure of Problem (TECM)

A key observation on Problem (TECM) is that p_{ik} in (4) is strictly convex with respect to s_{ik} when (ϵ_i, t_i) are given (the details can be referred to Proposition 1 in Section 4.1). Exploiting this important feature, we propose the following decomposition of Problem (TECM) as shown in Fig. 2 (we will explain the three subroutines shown in Fig. 2 in the next section).

3.3.1 *Subproblem to Optimize* $\mathbf{s}_i$ *Under Given* (ϵ_i, t_i)

Given ϵ_i and t_i, Problem (TECM) turns into a subproblem for optimizing $\mathbf{s}_i$ as follows:

$$\begin{aligned}
(\mathrm{TECM\text{-}Sub}): \quad & E_{i,(\epsilon_i,t_i)}^{\min} = \min \frac{S_i^{\mathrm{req}} - \sum_{k\in\mathcal{K}} s_{ik}}{V_i^{\mathrm{Loc}}}\rho_i^{\mathrm{Loc}} \\
&\qquad + t_i \sum_{k\in\mathcal{K}} \frac{n_{k\mathrm{E}} 2^{\frac{s_{ik}}{t_i W_k(1-\epsilon_i)}} - n_{k\mathrm{E}}}{\hat{g}_{ik} - \theta_{ik} 2^{\frac{s_{ik}}{t_i W_k(1-\epsilon_i)}}} \\
\text{subject to:} \quad & 0 \le s_{ik} \le s_{ik}^{\mathrm{upp}}, \forall k, && (11)\\
& S_i^{\mathrm{req}} - T_i^{\max} V_i^{\mathrm{Loc}} \le \sum_{k\in\mathcal{K}} s_{ik} \le S_i^{\mathrm{req}}, && (12)\\
\text{variables:} \quad & \mathbf{s}_i.
\end{aligned}$$

In constraint (11), s_{ik}^{upp}, which denotes the upper bound for s_{ik} under given (ϵ_i, t_i), is given by

$$\begin{aligned}
s_{ik}^{\mathrm{upp}} = \min\{ & S_i^{\mathrm{req}}, V_k\big(T_i^{\max} - t_i\big), \\
& (1-\epsilon_i) t_i W_k \log_2\left(\frac{\hat{g}_{ik}}{\theta_{ik}}\right)\}, \forall k \in \mathcal{K}.
\end{aligned} \tag{13}$$

Constraint (12) comes from constraints (8) and (10) before. It is noticed that in Problem (TECM-Sub), we use $E_{i,(\epsilon_i,t_i)}^{\min}$ to denote its optimal value, i.e., WD i's minimum energy consumption under the given tuple of (ϵ_i, t_i). In particular, we explicitly include the tuple of (ϵ_i, t_i) in the subscript of $E_{i,(\epsilon_i,t_i)}^{\min}$ to emphasize that this optimal value of Problem (TECM-Sub) depends on the given tuple of (ϵ_i, t_i).

3.3.2 Top-Problem to Optimize ϵ_i and t_i

With $E^{\min}_{i,(\epsilon_i,t_i)}$ from solving Problem (TECM-Sub), we then solve the following top-problem that jointly optimizes ϵ_i and t_i

$$\begin{aligned}(\text{TECM-Top}) : & E^{\min}_i = \min E^{\min}_{i,(\epsilon_i,t_i)} \\ \text{subject to: } & s^{\text{upp}}_{ik,(\epsilon_i,t_i)} \geq 0,\end{aligned} \tag{14}$$

$$\begin{aligned}& 0 \leq t_i \leq T^{\max}_i, \\ & \text{constraint } (9), \\ \text{variables: } & \epsilon_i \text{ and } t_i.\end{aligned} \tag{15}$$

Constraint (14) ensures that Problem (TECM-Sub) is feasible. Constraint (15) comes from constraint (10) before.

Thanks to the above decomposition, we can identify that Problem (TECM-Sub) is a strictly convex optimization problem, for which we can propose an efficient algorithm for obtaining the value of $E^{\min}_{i,(t_i,\epsilon_i)}$. The details are shown in the next section.

4 Proposed Algorithm to Solve Problem (TECM)

4.1 Analysis of Problem (TECM-Sub)

To efficiently solve Problem (TECM-Sub), we first identify the following important feature.

Proposition 1. *Given (t_i, ϵ_i), Subproblem (TECM-Sub) is a strictly convex problem.*

Proof. Please refer to Appendix A, which can be found on the Computer Society Digital Library at http://doi.ieeecomputersociety.org/10.1109/TMC.2021.3068902, for the details. □

The convexity in Proposition 1 enables us to use Karush-Kuhn-Tucher (KKT) conditions to solve Problem (TECM-Sub). Specifically, to deal with the coupling constraint (12), we introduce λ to denote the dual variable for $\sum_{k\in\mathcal{K}} s_{ik} \leq S^{\text{req}}_i$, and further use μ to denote the dual variable for $S^{\text{req}}_i - T^{\max}_i V^{\text{Loc}}_i \leq \sum_{k\in\mathcal{K}} s_{ik}$. Thus, we can derive the Lagrangian function $L(\mathbf{s}_i, \lambda, \mu)$ as shown in (16)

$$\begin{aligned}L(\mathbf{s}_i, \lambda, \mu) = & \sum_{k\in\mathcal{K}} t_i n_{k\text{E}} \frac{2^{\frac{s_{ik}}{t_i W_k(1-\epsilon_i)}} - 1}{\hat{g}_{ik} - \theta_{ik} 2^{\frac{s_{ik}}{t_i W_k(1-\epsilon_i)}}} \\ & + \frac{S^{\text{req}}_i - \sum_{k\in\mathcal{K}} s_{ik}}{V^{\text{Loc}}_i} \rho^{\text{Loc}}_i + \lambda \left(\sum_{k\in\mathcal{K}} s_{ik} - S^{\text{req}}_i \right) \\ & + \mu \left(S^{\text{req}}_i - \sum_{k\in\mathcal{K}} s_{ik} - T^{\max}_i V^{\text{Loc}}_i \right).\end{aligned} \tag{16}$$

Furthermore, by setting $\frac{dL(\mathbf{s}_i,\lambda,\mu)}{ds_{ik}} = 0$, we obtain the following quadratic equation:

$$\frac{n_{k\text{E}} \ln 2 (\hat{g}_{ik} - \theta_{ik}) z_{ik}}{W_k(1-\epsilon_i)(\hat{g}_{ik} - \theta_{ik} z_{ik})^2} = \Gamma_i(\lambda, \mu), \tag{17}$$

where z_{ik} is an auxiliary variable defined as

$$z_{ik} = 2^{\frac{s_{ik}}{t_i W_k(1-\epsilon_i)}}, \tag{18}$$

and the auxiliary function $\Gamma_i(\lambda, \mu)$ is defined as

$$\Gamma_i(\lambda, \mu) = \frac{\rho^{\text{Loc}}_i}{V^{\text{Loc}}_i} + \mu - \lambda, \tag{19}$$

to capture the impact of the dual variables (λ, μ).

Notice that the auxiliary variable z_{ik} is required to meet the following condition due to constraint (5) before

$$z_{ik} \leq \frac{\hat{g}_{ik}}{\theta_{ik}}. \tag{20}$$

In particular, an important feature of Eq. (17) is as follows.

Proposition 2. *Given (λ, μ), Eq. (17) always has a unique root which satisfies constraint (20), and the value of this unique root is given by*

$$z^{\text{root}}_{ik} = \frac{B - \sqrt{\Theta}}{2A}, \tag{21}$$

where parameters A and B are respectively given by

$$A = \Gamma_i(\lambda, \mu) W_k (1 - \epsilon_i) \theta^2_{ik}, \tag{22}$$

$$B = 2\Gamma_i(\lambda, \mu) W_k (1 - \epsilon_i) \hat{g}_{ik} \theta_{ik} + n_{k\text{E}} (\hat{g}_{ik} - \theta_{ik}) \ln 2. \tag{23}$$

Meanwhile, parameter Θ is given by

$$\begin{aligned}\Theta = & \left(n_{k\text{E}} (\hat{g}_{ik} - \theta_{ik}) \ln 2\right)^2 \\ & + 4\Gamma_i(\lambda, \mu) W_k (1 - \epsilon_i) \hat{g}_{ik} \theta_{ik} n_{k\text{E}} (\hat{g}_{ik} - \theta_{ik}) \ln 2.\end{aligned} \tag{24}$$

Proof. After some manipulations, Eq. (17) can be equivalently transformed into a quadratic equation as follows:

$$A z^2_{ik} - B z_{ik} + C = 0, \tag{25}$$

where parameters A and B are given in (22) and (23) respectively, and parameter $C = \Gamma_i(\lambda, \mu) W_k (1 - \epsilon_i) \hat{g}^2_{ik}$. In particular, it can be identified that parameter Θ in Eq. (24) satisfies the following condition:

$$\Theta = B^2 - 4AC > 0. \tag{26}$$

Therefore, the quadratic equation in (25) always has two roots. Moreover, it can be identified that only the smaller root, i.e., z^{root}_{ik} given in Eq. (21), satisfies condition (20). We thus finish the proof. □

With (21), we can obtain the unique value of s^{root}_{ik} that can ensure $\frac{dL(\mathbf{s}_i,\lambda,\mu)}{ds_{ik}} = 0$ as follows:

$$s^{\text{root}}_{ik} = (1 - \epsilon_i) t_i W_k \log_2(z^{\text{root}}_{ik}). \tag{27}$$

Recall that due to function $\Gamma_i(\lambda, \mu)$ in (19), both z^{root}_{ik} (in Eq. (21)) and s^{root}_{ik} (in Eq. (27)) depend on the values of (λ, μ). Moreover, we have the following result regarding the impact of (λ, μ).

Proposition 3. *Given (t_i, ϵ_i), the value of s_{ik}^{root} decreases in λ, and increases in μ.*

Proof. Please refer to Appendix B, available in the online supplemental material, for the details. □

Notice that the monotonic feature illustrated in Proposition 3 will be used in our algorithmic design for solving Problem (TECM-Sub) in the next subsection.

An important feature of Problem (TECM-Sub) is that at the optimum, the dual variables λ and μ cannot be positive at the same time. Therefore, let $\mathbf{s}_i^*$ denote the optimal solution of Problem (TECM-Sub). By considering different combinations of (λ, μ), we obtain the only three possible cases for $\mathbf{s}_i^*$ to occur, which are illustrated in the following proposition.

Proposition 4. *Given (t_i, ϵ_i), there exist three possible cases for the optimal solution $\mathbf{s}_i^*$ of Problem (TECM-Sub) to occur. The details are as follows.*

- (Case-I): *the optimal solution $\mathbf{s}_i^*$ occurs when $\sum_{k\in\mathcal{K}} s_{ik}^* = S_i^{\text{req}}$ (i.e., the right-hand-side of constraint (12) is strictly binding). In this case, $\mu^* = 0$ holds, and there exists a unique value of $\lambda^* \le \lambda^{\text{upp}}$ such that $\sum_{k\in\mathcal{K}} s_{ik}^* = S_i^{\text{req}}$.*
- (Case-II): *the optimal solution $\mathbf{s}_i^*$ occurs when $\sum_{k\in\mathcal{K}} s_{ik}^* = S_i^{\text{req}} - T_i^{\max} V_i^{\text{Loc}}$ (i.e., the left-hand-side of constraint (12) is strictly binding). In this case, $\lambda^* = 0$ holds, and there exists a unique value of μ^* such that $\sum_{k\in\mathcal{K}} s_{ik}^* = S_i^{\text{req}} - T_i^{\max} V_i^{\text{Loc}}$,*
- (Case-III): *the optimal solution $\mathbf{s}_i^*$ occurs when $S_i^{\text{req}} - T_i^{\max} V_i^{\text{Loc}} < \sum_{k\in\mathcal{K}} s_{ik}^* < S_i^{\text{req}}$ holds. In this case, there exist both $\lambda^* = 0$ and $\mu^* = 0$.*

Proof. Please refer to Appendix C, available in the online supplemental material, for the details. □

4.2 Proposed Algorithm for Solving Problem (TECM)

With Proposition 4, we first design three subroutines for the aforementioned Case-I, Case-II, and Case-III, which together solve Problem (TECM-Sub). The details are as follows.

Subroutine-I aims at finding $\mathbf{s}_i^*$ under Case-I, which works as follows. Based on Case-I in Proposition 4 and the monotonic feature in Proposition 3, we adopt the bisection search (i.e., the whole-loop from Step 2 to Step 16) to find the value of λ^* such that $\sum_{k\in\mathcal{K}} s_{ik}^* = S_i^{\text{req}}$. In particular, we set $\lambda^{\text{upp}} = \frac{\rho_i^{\text{Loc}}}{V_i^{\text{Loc}}}$ to ensure that $\Gamma_i(\lambda, 0) \ge 0$, and set λ^{low} as a small negative number.

Similarly to Subroutine-I, we propose Subroutine-II, which executes a bisection search on μ, for finding $\mathbf{s}_i^*$ such that $\sum_{k\in\mathcal{K}} s_{ik}^* = S_i^{\text{req}} - T_i^{\max} V_i^{\text{Loc}}$. In particular, we set $\mu^{\text{low}} = -\frac{\rho_i^{\text{Loc}}}{V_i^{\text{Loc}}}$ to ensure that $\Gamma_i(0, \mu) \ge 0$, and set μ^{upp} as a large positive number.

Finally, we propose Subroutine-III for finding $\mathbf{s}_i^*$ under Case-III. Specifically, we derive the values of z_{ik}^{root} and $s_{ik}^{\text{root}}, \forall k \in \mathcal{K}$ based on (21) and (27), respectively, when $\lambda = 0$ and $\mu = 0$. Notice that according to constraint (12), Case-III is viable only if the condition $S_i^{\text{req}} - T_i^{\max} V_i^{\text{Loc}} < \sum_{k\in\mathcal{K}} \max\{\min\{s_{ik}^{\text{root}}, s_{ik}^{\text{upp}}\}, 0\} < S_i^{\text{req}}$ holds.

Subroutine-I To Find $\mathbf{s}_i^*$ Under Case-I

1: **Initialization:** Set $\mu = 0$, $\overline{\lambda} = \lambda^{\text{upp}}$ and $\underline{\lambda} = \lambda^{\text{low}}$. Set the tolerable computation-error γ.
2: **while** True **do**
3: Update $\lambda^{\text{cur}} = \frac{1}{2}(\overline{\lambda} + \underline{\lambda})$.
4: Given $(\lambda^{\text{cur}}, \mu)$, use (21) and (27) to obtain the values of z_{ik}^{root} and $s_{ik}^{\text{root}}, \forall k \in \mathcal{K}$.
5: **if** $\sum_{k\in\mathcal{K}} \max\{\min\{s_{ik}^{\text{root}}, s_{ik}^{\text{upp}}\}, 0\} > S_i^{\text{req}} + \gamma$ **then**
6: Set $\underline{\lambda} = \lambda^{\text{cur}}$.
7: **else**
8: **if** $\sum_{k\in\mathcal{K}} \max\{\min\{s_{ik}^{\text{root}}, s_{ik}^{\text{upp}}\}, 0\} < S_i^{\text{req}} - \gamma$ **then**
9: Set $\overline{\lambda} = \lambda^{\text{cur}}$.
10: **else**
11: Set $s_{ik}^* = \max\{\min\{s_{ik}^{\text{root}}, s_{ik}^{\text{upp}}\}, 0\}, \forall k \in \mathcal{K}$.
12: Compute the value of $E_{i,(t_i,\epsilon_i)}^{\min}$ based on $\mathbf{s}_i^*$.
13: Go to Step 17.
14: **end if**
15: **end if**
16: **end while**
17: **Output**: $\mathbf{s}_i^*$ and the corresponding $E_{i,(t_i,\epsilon_i)}^{\min}$.

Subroutine-II To Find $\mathbf{s}_i^*$ Under Case-II

1: **Initialization:** Set $\lambda = 0$, $\overline{\mu} = \mu^{\text{upp}}$ and $\underline{\mu} = \mu^{\text{low}}$. Set the tolerable computation-error γ.
2: **while** True **do**
3: Update $\mu^{\text{cur}} = \frac{1}{2}(\overline{\mu} + \underline{\mu})$.
4: Given $(\lambda, \mu^{\text{cur}})$, use (21) and (27) to obtain the values of z_{ik}^{root} and $s_{ik}^{\text{root}}, \forall k \in \mathcal{K}$.
5: **if** $\sum_{k\in\mathcal{K}} \max\{\min\{s_{ik}^{\text{root}}, s_{ik}^{\text{upp}}\}, 0\} > S_i^{\text{req}} - T_i^{\max} V_i^{\text{Loc}} + \gamma$ **then**
6: Set $\overline{\mu} = \mu^{\text{cur}}$.
7: **else**
8: **if** $\sum_{k\in\mathcal{K}} \max\{\min\{s_{ik}^{\text{root}}, s_{ik}^{\text{upp}}\}, 0\} < S_i^{\text{req}} - T_i^{\max} V_i^{\text{Loc}} - \gamma$ **then**
9: Set $\underline{\mu} = \mu^{\text{cur}}$.
10: **else**
11: Set $s_{ik}^* = \max\{\min\{s_{ik}^{\text{root}}, s_{ik}^{\text{upp}}\}, 0\}, \forall k \in \mathcal{K}$.
12: Compute the value of $E_{i,(t_i,\epsilon_i)}^{\min}$ based on $\mathbf{s}_i^*$.
13: Go to Step 17.
14: **end if**
15: **end if**
16: **end while**
17: **Output**: $\mathbf{s}_i^*$ and the corresponding $E_{i,(t_i,\epsilon_i)}^{\min}$.

Subroutine-III To Find $\mathbf{s}_i^*$ Under Case-III

1: **Initialization:** Set $\lambda = 0$, and $\mu = 0$. Initialize $\mathbf{s}_i^* = \emptyset$, and $E_{i,(t_i,\epsilon_i)}^{\min}$ as an extremely large yet positive number.
2: Given (λ, μ), use (21) and (27) to obtain the values of z_{ik}^{root} and $s_{ik}^{\text{root}}, \forall k \in \mathcal{K}$.
3: **if** $S_i^{\text{req}} - T_i^{\max} V_i^{\text{Loc}} < \sum_{k\in\mathcal{K}} \max\{\min\{s_{ik}^{\text{root}}, s_{ik}^{\text{upp}}\}, 0\} < S_i^{\text{req}}$ **then**
4: Update $s_{ik}^* = \max\{\min\{s_{ik}^{\text{root}}, s_{ik}^{\text{upp}}\}, 0\}, \forall k \in \mathcal{K}$.
5: Compute the value of $E_{i,(t_i,\epsilon_i)}^{\min}$ based on $\mathbf{s}_i^*$.
6: **end if**
7: **Output**: $\mathbf{s}_i^*$ and the corresponding $E_{i,(t_i,\epsilon_i)}^{\min}$.

With Subroutine-I, Subroutine-II, and Subroutine-III, we propose Sub-Algorithm to solve Problem (TECM-Sub).

Specifically, with the given tuple of (t_i, ϵ_i), we can obtain $\{s_{ik}^{\rm upp}\}_{k\in\mathcal{K}}$ according to (13). If $\sum_{k\in\mathcal{K}} s_{ik}^{\rm upp} < S_i^{\rm req} - T_i^{\max}V_i^{\rm Loc}$, then Problem (TECM-Sub) is infeasible under the current (t_i, ϵ_i). If $S_i^{\rm req} - T_i^{\max}V_i^{\rm Loc} \le \sum_{k\in\mathcal{K}} s_{ik}^{\rm upp} < S_i^{\rm req}$, we only need to evaluate Case-II and Case-III (i.e., from Step 5 to Step 8), and compare with the consequent outputs of the two cases. If $\sum_{k\in\mathcal{K}} s_{ik}^{\rm upp} \ge S_i^{\rm req}$, then we need to evaluate Case-I, Case-II, and Case-III (i.e., from Step 10 to Step 15), and compare with the consequent outputs of the three cases. Eventually, Sub-Algorithm outputs WD i's optimal offloading solution $\mathbf{s}_i^*$ under the given tuple of (t_i, ϵ_i) and the corresponding $E_{i,(t_i,\epsilon_i)}^{\min}$. We thus complete solving Problem (TECM-Sub).

Sub-Algorithm To Solve Problem (TECM-Sub) and Find $\mathbf{s}_i^*$ and $E_{i,(t_i,\epsilon_i)}^{\min}$

1: **Initialization:** Given (t_i, ϵ_i), use (13) to compute $s_{ik}^{\rm upp}, \forall k \in \mathcal{K}$. Set $\text{flag} = 0$. Set the current best value CBV as a very large number, and set the current best solution $\text{CBS} = \emptyset$.
2: **if** $\sum_{k\in\mathcal{K}} s_{ik}^{\rm upp} < S_i^{\rm req} - T_i^{\max}V_i^{\rm Loc}$ **then**
3: Problem (TECM-Sub) is infeasible.
4: **else if** $S_i^{\rm req} - T_i^{\max}V_i^{\rm Loc} \le \sum_{k\in\mathcal{K}} s_{ik}^{\rm upp} < S_i^{\rm req}$ **then**
5: Invoke Subroutine-II.
6: If $E_{i,(t_i,\epsilon_i)}^{\min}$ output by Subroutine-II satisfies $E_{i,(t_i,\epsilon_i)}^{\min} < \text{CBV}$, then update $\text{CBS} = \mathbf{s}_i^*$ and $\text{CBV} = E_{i,(t_i,\epsilon_i)}^{\min}$.
7: Invoke Subroutine-III.
8: If $E_{i,(t_i,\epsilon_i)}^{\min}$ output by Subroutine-III satisfies $E_{i,(t_i,\epsilon_i)}^{\min} < \text{CBV}$, then update $\text{CBS} = \mathbf{s}_i^*$ and $\text{CBV} = E_{i,(t_i,\epsilon_i)}^{\min}$.
9: **else**
10: Invoke Subroutine-I.
11: If $E_{i,(t_i,\epsilon_i)}^{\min}$ output by Subroutine-I satisfies $E_{i,(t_i,\epsilon_i)}^{\min} < \text{CBV}$, then update $\text{CBS} = \mathbf{s}_i^*$ and $\text{CBV} = E_{i,(t_i,\epsilon_i)}^{\min}$.
12: Invoke Subroutine-II.
13: If $E_{i,(t_i,\epsilon_i)}^{\min}$ output by Subroutine-II satisfies $E_{i,(t_i,\epsilon_i)}^{\min} < \text{CBV}$, then update $\text{CBS} = \mathbf{s}_i^*$ and $\text{CBV} = E_{i,(t_i,\epsilon_i)}^{\min}$.
14: Invoke Subroutine-III.
15: If $E_{i,(t_i,\epsilon_i)}^{\min}$ output by Subroutine-III satisfies $E_{i,(t_i,\epsilon_i)}^{\min} < \text{CBV}$, then update $\text{CBS} = \mathbf{s}_i^*$ and $\text{CBV} = E_{i,(t_i,\epsilon_i)}^{\min}$.
16: **end if**
17: **Output**: Output the optimal value of Problem (TECM-Sub) as $E_{i,(t_i,\epsilon_i)}^{\min} = \text{CBV}$ and the corresponding optimal workload-offloading $\mathbf{s}_i^* = \text{CBS}$ (notice that $\mathbf{s}_i^* = \emptyset$ means that Problem (TECM-Sub) is infeasible).

After solving Problem (TECM-Sub), we next continue to solve Problem (TECM-Top). The difficulty in solving Problem (TECM-Top) is that we cannot express $E_{i,(t_i,\epsilon_i)}^{\min}$ analytically. As a result, we cannot adopt conventional gradient-based schemes to characterize the optimality condition for Problem (TECM-Top). Nevertheless, constraint (9) ensures that $\epsilon_i \in [0, \epsilon_i^{\max}]$, and constraint (15) ensures that $t_i \in [0, T_i^{\max}]$. In other words, both t_i and ϵ_i fall within the respectively given intervals independent on other parameters. This feature thus allows us to adopt a two-dimensional line-search method (with a small step-size) for solving Problem (TECM-Top) numerically. The details are shown in our proposed Top-Algorithm. Specifically, for each tuple of (t_i, ϵ_i) being evaluated, we invoke Sub-Algorithm to obtain $\mathbf{s}_i^*$ and the corresponding $E_{i,(t_i,\epsilon_i)}^{\min}$, and further update the current best solution denoted by CBS consequently.

With the given small step-size Δ, a total number of $\frac{1}{\Delta^2} T_i^{\max}\epsilon_i^{\max}$ iterations are required by our Top-Algorithm. Meanwhile, for each given tuple of (t_i, ϵ_i), Sub-Algorithm requires no more than $\left(\log_2\left(\frac{\lambda^{\rm upp}-\lambda^{\rm low}}{\gamma}\right) + \log_2\left(\frac{\mu^{\rm upp}-\mu^{\rm low}}{\gamma}\right)\right)$ rounds of iterations due to the bisection-search on the dual variables, with γ being the tolerable computation-error. As a result, the overall complexity of our Top-Algorithm can be given by $\frac{T_i^{\max}\epsilon_i^{\max}}{\Delta^2}\left(\log_2\left(\frac{\lambda^{\rm upp}-\lambda^{\rm low}}{\gamma}\right) + \log_2\left(\frac{\mu^{\rm upp}-\mu^{\rm low}}{\gamma}\right)\right)$. Moreover, thanks to exploiting the optimality conditions illustrated in Proposition 4, our Sub-Algorithm is guaranteed to converge to the optimal solution of the subproblem under the given tuple of (t_i, ϵ_i). As a result, our Top-Algorithm is guaranteed to converge to the optimal solution of the original Problem (TECM) by using a sufficiently small step-size in the line-search.

Top-Algorithm To Solve Problem (TECM-Top) Find $(\mathbf{s}_i^*, t_i^*, \epsilon_i^*)$ and $E_i^{\min}$

1: **Initialization:** Set the current best value CBV as a very large number, and set the current best solution $\text{CBS} = \emptyset$. Set $\text{flag} = 0$.
2: **for** $t_i^{\rm temp} = 0 : \Delta : T_i^{\max}$ **do**
3: **for** $\epsilon_i^{\rm temp} = 0 : \Delta : \epsilon_i^{\max}$ **do**
4: Given $(t_i^{\rm temp}, \epsilon_i^{\rm temp})$, invoke Sub-Algorithm.
5: **if** Problem (TECM-Sub) is feasible **then**
6: Update $\text{flag} = 1$.
7: If $E_{i,(t_i^{\rm temp},\epsilon_i^{\rm temp})}^{\min}$ (which is output by Sub-Algorithm) satisfies $E_{i,(t_i^{\rm temp},\epsilon_i^{\rm temp})}^{\min} < \text{CBV}$, then update $\text{CBS} = (\mathbf{s}_i^*, t_i^{\rm temp}, \epsilon_i^{\rm temp})$ and $\text{CBV} = E_{i,(t_i^{\rm temp},\epsilon_i^{\rm temp})}^{\min}$.
8: **end if**
9: **end for**
10: **end for**
11: **Output**: If $\text{flag} = 0$, output that Problem (TECM) is infeasible. Otherwise, output the optimal value of Problem (TECM) as $E_i^{\min} = \text{CBV}$ and the optimal solution of Problem (TECM) as $(\mathbf{s}_i^*, t_i^*, \epsilon_i^*) = \text{CBS}$.

4.3 Numerical Results for the Single-WD Scenario

In this subsection, we present simulation results to demonstrate the performance of our proposed algorithm for solving Problem (TECM). Specifically, we setup an one-WD 3-ECS scenario as follows. The WD is randomly generated within a plane within the center at (0,0) and the radius of 200m, and the locations of the ECSs are distributed uniformly on a circle of radius 500m. Similar to [17], [20], we adopt the path-loss model to generate the channel power gains from the WD to the ECSs, which accounts for both the path-loss effect and the fading effect. Specifically, the randomly generated channel power gains from WD i to the three ECSs used in this section are $\{g_{i1}, g_{i2}, g_{i3}\} = [14.448, 4.7100, 4.1374] \times 10^{-8}$. In addition, we set the average eavesdropping-path gain $\alpha_{i\rm E} = 1 \times 10^{-9}$. For WD i, we set its secrecy-outage requirement $\epsilon_i^{\max} = 0.2$, latency-requirement $T_i^{\max} = 2.5$ seconds. Meanwhile, we set $V_i^{\rm Loc} = 1$ Mbps and $\rho_i^{\rm Loc} = 0.02$. For each ECS k, we set the computing-rate $V_k = 4$ Mbps and the channel bandwidth $W_k = 5$ MHz. All the following testings are performed on a PC with Intel Core i5-8250U of CPU 1.60 GHz.

Fig. 3 shows the convergence example of our Subroutine-I and Subroutine-II when $t_i = 1.25$sec and $\epsilon_i = 0.01$. Specifically, subplot Fig. 3a shows the convergence of λ under Case-I, and subplot Fig. 3b shows the convergence

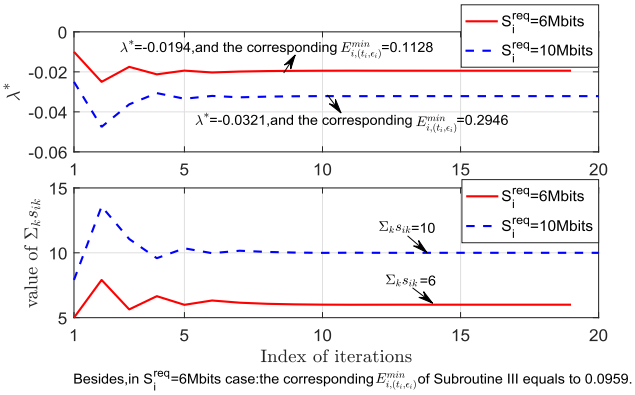

(a) Top-subplot: λ^*. Bottom-subplot: value of $\sum_k s_{ik}$.

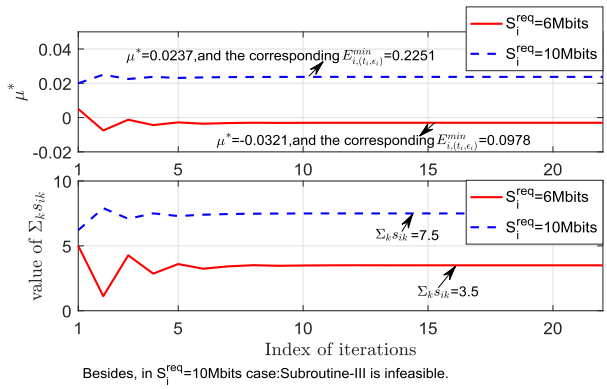

(b) Top-subplot: μ^*. Bottom-subplot: value of $\sum_k s_{ik}$.

Fig. 3. Convergence examples of Subroutine-I and Subroutine-II under given (t_i, ϵ_i).

of μ under Case-II. The results verify the effectiveness of our proposed subroutines for solving Problem (TECM-Sub). Furthermore, Fig. 4 provides a detailed example of executing Top-Algorithm which executes a two-dimension search on (ϵ_i, t_i) for minimizing WD i's total energy consumption.

Fig. 5 verifies the effectiveness and computational efficiency of our proposed algorithm for solving Problem (TECM) by comparing with LINGO (i.e., a commercial optimization software [43]). Specifically, LINGO's global-solver adopts the classic algorithm of the branch-and-bound to address the non-convexity of the optimization problem and thus can provide the optimal solution for our Problem (TECM) as a benchmark. The results in Fig. 5a show that our Top-Algorithm can achieve the solutions extremely close to the global optimum solution from LINGO. Meanwhile, the results in Fig. 5b further validate the computational efficiency of our Top-algorithm. Thanks to exploiting the decomposition structure (illustrated in Section 3.3) and the efficient Subroutines I to III based on Proposition 4, our Top-algorithm can significantly reduce the computational time in comparison with the global-solver of LINGO, as shown in Fig. 5b. It is worth pointing out that although Fig. 5 mainly shows the results under $K = 3$, the corresponding results under $K = 5$ and $K = 7$ also demonstrate the similar performance advantages of our proposed algorithm, which, however, are not presented here due to the limited space.

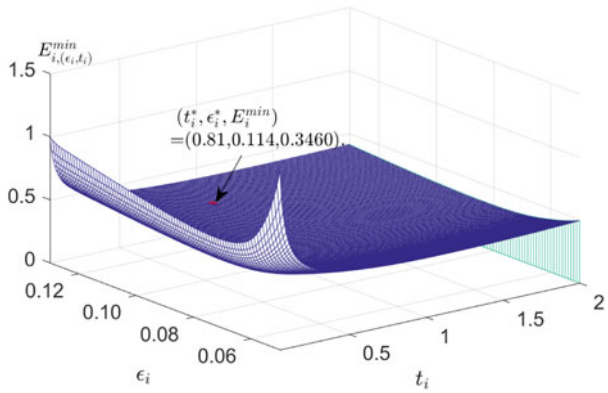

Fig. 4. An example of executing Top-Algorithm for minimizing $E^{\min}_{i,(t_i,\epsilon_i)}$.

Fig. 6 shows the advantage of our optimal multi-offloading scheme in comparison with a conventional fixed offloading scheme in which WD i offloads a fixed portion of its required workload to each ECS. For instance, "5 percent to each ECS" in Fig. 6 means that WD i offloads 5 percent of its total workload to each ECS. The results in Fig. 6 validate that our proposed scheme can effectively reduce WD i's total energy consumption while satisfying both the secrecy-requirement and latency-requirement, by properly optimizing the WD's multi-access offloading.

It is noticed that the secrecy-requirement of the WD influences the optimal offloading solution. Thus, we evaluate this impact with the results shown in Fig. 7, in which we vary $\epsilon_i^{\max}$ from 0.05 (i.e., a stringent secrecy-requirement) to 0.25 (i.e., a loose secrecy-requirement). The left-subplot shows the resulting total energy consumption, and the right subplot shows the corresponding total offloaded workloads from WD i. The results demonstrate that a loose secrecy-requirement can yield a smaller total energy consumption, since it provides a larger flexibility in WD i's offloading transmission and thus enables WD i to offload more computation-workloads to the ECSs. These results are consistent with the intuitions well.

5 Extension to the Multi-WD Scenario

Based on our study on the single-WD scenario in Sections 3 and 4, we further investigate a more general yet complicated scenario of multi-WDs' multi-access offloading subject to the eavesdropping-attack as shown in Fig. 8. Specifically, we consider a group of WDs denoted by $\mathcal{I} = \{1, 2, \ldots, I\}$ which offload their computation-workloads to the ECSs sequentially and occupy the ECSs' computation-resources in a time division manner (TDM). In other words, a hybrid FDMA and TDM is used for the multi-WDs scenario, in which different WDs use TDM for their respective offloading transmissions in sequence, and each individual WD adopts FDMA for sending its offloaded workloads to different ECSs simultaneously.

In the multi-WDs scenario, the latency of different WDs in completing their respective tasks are coupled with each other. Specifically, let us consider a detailed example of WD i and WD j executing their respective computation offloading, with WD i right prior to WD j. In this case, WD j can

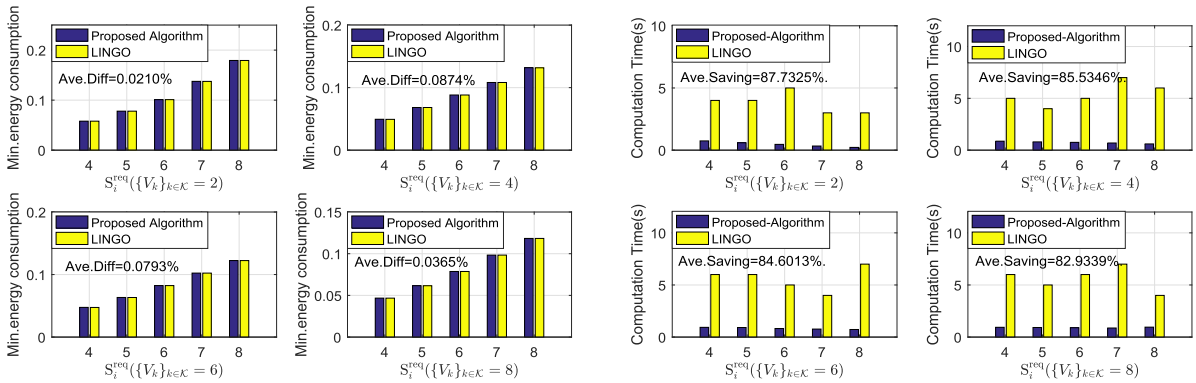

(a) Effectiveness of Proposed Algorithm (b) Efficiency of Proposed Algorithm

Fig. 5. Illustration of effectiveness and computational efficiency of Top-Algorithm in comparison with LINGO.

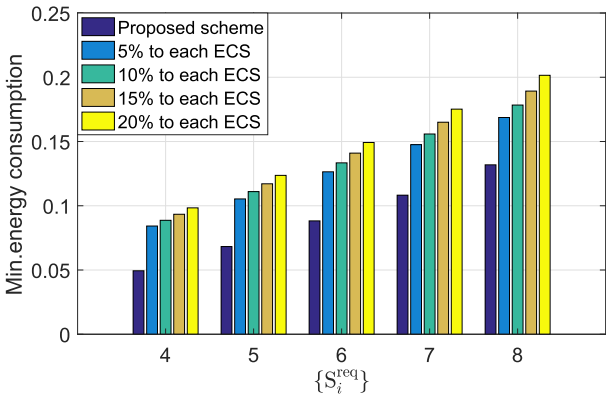

Fig. 6. Comparison with the heuristic fixed offloading scheme.

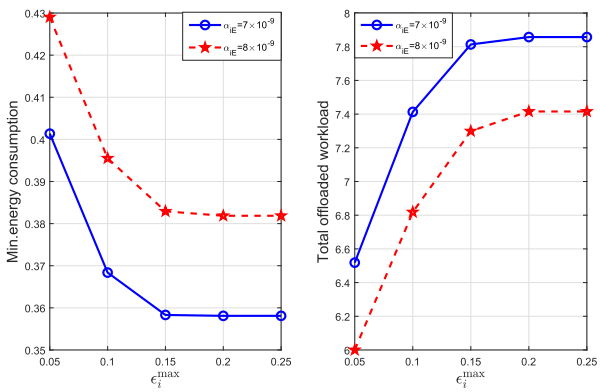

Fig. 7. Impact of the secrecy-requirement on the optimal offloading solution. Left-subplot: total energy consumption. Right-subplot: total offloaded workloads.

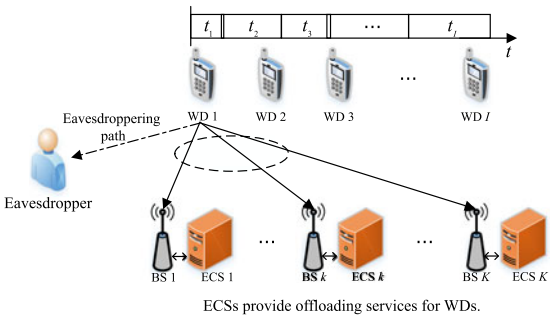

Fig. 8. Illustrative system model of the multi-WDs' multi-access offloading subject to the eavesdropping-attack.

only start its offloading transmission after WD i completes its offloading transmission. Moreover, WD j's offloaded workload to each ECS k can only be processed after ECS k completes the offloaded workload of WD i. As a result, the WDs' ordering will influence each WD j's overall latency in completing its task, and we need to re-consider how to quantify each WD's latency. Based on this motivation, in the multi-WDs scenario, we investigate the joint optimization of the WDs' offloading-ordering, as well as each WD's transmission-duration, offloaded workload, and secrecy provisioning, with the objective of minimizing the total energy consumption of all WDs.

5.1 Modeling of Multi-WDs Offloading

In the multi-WDs scenario, different WDs sequentially send their respective offloaded workloads to the ECSs, and occupy the ECSs' computation-resources for processing. Therefore, the latency of different WDs in completing their required workloads are strongly coupled. To model this relationship, we introduce a mapping $\boldsymbol{\pi}$ to denote an offloading-ordering of the WDs in $\mathcal{I}$, i.e., $\pi(i)$ means that WD i is the $\pi(i)$th one to execute the computation offloading. Thus, $\pi(i)-1$ denotes the WD which executes the computation offloading right in front of WD i in ordering $\boldsymbol{\pi}$.

To save the time resource in occupying wireless channel, we consider that each WD i starts its offloading-transmission immediately when WD $\pi(i)-1$ completes the offloading-transmission. Specifically, we use variable $\alpha_{\pi(i)}$ to denote the time-instance when WD i completes its offloading transmission and use variable $\alpha_{\pi(i)-1}$ to denote the time-instance when the WD, which is in front of WD i in ordering $\boldsymbol{\pi}$, completes the offloading transmission. Therefore, as illustrated by the the example in Fig. 9, the value of $\alpha_{\pi(i)}$ can be calculated as

$$\alpha_{\pi(i)} = \alpha_{\pi(i)-1} + t_i, \forall i \in \mathcal{I}, \tag{28}$$

where $\alpha_0 = 0$ for the sake of initialization.

Furthermore, we introduce variable $\beta_{\pi(i),k}$ to denote the time-instance when ECS k completes processing the offloaded workload from WD i, and use $\beta_{\pi(i)-1,k}$ to denote the time-instance when ECS k completes processing the offloaded workload from the WD which is in front of WD i in the ordering π. Therefore, as illustrated by the example in Fig. 9, the value of $\beta_{\pi(i),k}$ can be calculated as

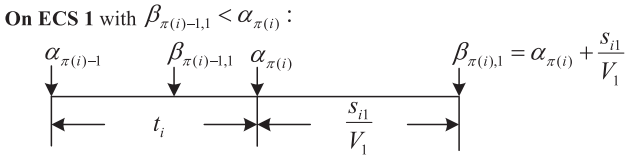

(a) Illustrative example of $\beta_{\pi(i)-1,1} < \alpha_{\pi(i)}$ on ECS-1

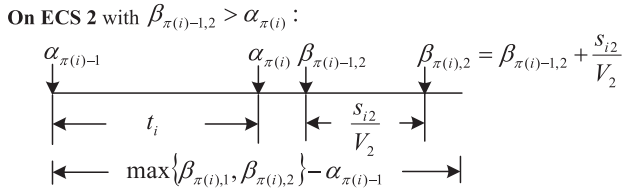

(b) Illustrative example of $\beta_{\pi(i)-1,2} > \alpha_{\pi(i)}$ on ECS-2

Fig. 9. An illustrative example of WD i's offloading under a 2-ECSs scenario, in which we assume $\beta_{\pi(i)-1,1} < \alpha_{\pi(i)}$ on ECS-1 (in subplot (a)), and $\beta_{\pi(i)-1,2} > \alpha_{\pi(i)}$ on ECS-2 (in subplot (b)).

$$\beta_{\pi(i),k} = \max\{\beta_{\pi(i)-1,k}, \alpha_{\pi(i)}\} + \frac{s_{ik}}{V_k}, \forall i \in \mathcal{I}, k \in \mathcal{K}, \tag{29}$$

where $\beta_{0,k} = 0, \forall k \in \mathcal{K}$ for the sake of initialization.

With $\{\alpha_{\pi(i)}\}_{i\in\mathcal{I}}$ and $\{\beta_{\pi(i),k}\}_{i\in\mathcal{I},k\in\mathcal{K}}$ respectively modeled in (28) and (29) above, we can express the overall latency for WD i, which is the $\pi(i)$th one to execute offloading in ordering $\boldsymbol{\pi}$, to complete its required workload as follows:

$$L_i^{\text{mul}} = \max\{\max_{k\in\mathcal{K}}\{\beta_{\pi(i),k}\} - \alpha_{\pi(i)-1}, \frac{S_i^{\text{req}} - \sum_{k\in\mathcal{K}} s_{ik}}{V_i^{\text{Loc}}}\}, \forall i \in \mathcal{I}. \tag{30}$$

Specifically, $\frac{S_i^{\text{req}} - \sum_{k\in\mathcal{K}} s_{ik}}{V_i^{\text{Loc}}}$ denotes the latency for WD i to complete its remaining workload locally, and $\max_{k\in\mathcal{K}}\{\beta_{\pi(i),k}\} - \alpha_{\pi(i)-1}$ denotes the latency for WD i's multi-access computation offloading via all ECSs as illustrated in Fig. 9. Specifically, Fig. 9 illustrates an example of $\{\alpha_{\pi(i)}\}_{i\in\mathcal{I}}$ and $\{\beta_{\pi(i),k}\}_{i\in\mathcal{I},k\in\mathcal{K}}$, when WD i executes the multi-access offloading towards to two ESCs, with $\beta_{\pi(i)-1,1} < \alpha_{\pi(i)}$ on ECS-1 and $\beta_{\pi(i)-1,2} > \alpha_{\pi(i)}$ on ECS-2.

Before leaving this subsection, we emphasize that with $\{t_i\}_{i\in\mathcal{I}}$ and $\{s_{ik}\}_{i\in\mathcal{I},k\in\mathcal{K}}$, we can use (28) and (29) to iteratively calculate the time-instances $\{\alpha_{\pi(i)}\}_{i\in\mathcal{I}}$ and $\{\beta_{\pi(i),k}\}_{i\in\mathcal{I},k\in\mathcal{K}}$, respectively, according to the ordering $\boldsymbol{\pi}$, and further use (30) to obtain the corresponding overall-latency for each WD i. In other words, $\{\alpha_{\pi(i)}\}_{i\in\mathcal{I}}$ and $\{\beta_{\pi(i),k}\}_{i\in\mathcal{I},k\in\mathcal{K}}$ can be treated as the auxiliary variables which depend on *the core variables* $\{t_i\}_{i\in\mathcal{I}}$ and $\{s_{ik}\}_{i\in\mathcal{I},k\in\mathcal{K}}$.

5.2 Problem Formulation for the Multi-WDs Scenario

Based on the above modeling of each WD's latency, we formulate a joint optimization of the offloading ordering $\boldsymbol{\pi}$ of all WDs, as well as each WD i's multi-access workload offloading $\mathbf{s}_i$, the transmission-duration t_i, and the secrecy-provisioning ϵ_i, with the objective of minimizing the total energy consumption of all WDs, while subject to each WD's latency-requirement and secrecy-requirement. The details are shown in the following problem formulation:

$$\text{(MultiWD)}: \min \sum_{i\in\mathcal{I}} \left\{ \frac{S_i^{\text{req}} - \sum_{k\in\mathcal{K}} s_{ik}}{V_i^{\text{Loc}}} \rho_i^{\text{Loc}} + t_i \sum_{k\in\mathcal{K}} p_{ik} \right\}$$

$$\text{subject to: } 0 \le s_{ik} \le S_i^{\text{req}}, \forall i \in \mathcal{I}, \forall k \in \mathcal{K}, \tag{31}$$

$$\sum_{k\in\mathcal{K}} s_{ik} \le S_i^{\text{req}}, \forall i \in \mathcal{K}, \tag{32}$$

$$0 \le \epsilon_i \le \epsilon_i^{\max}, \forall i \in \mathcal{I}, \tag{33}$$

$$L_i^{\text{mul}} \le T_i^{\max}, \forall i \in \mathcal{I}, \tag{34}$$

$$\text{constraints } (4), (5), \text{ and } (30),$$

$$\text{variables: } \boldsymbol{\pi}, \text{ and } (\{s_{ik}\}_{k\in\mathcal{K}}, t_i, \epsilon_i), \forall i \in \mathcal{I}.$$

Notice that in Problem (MultiWD), constraint (34) ensures that each WD i's latency in the multi-WDs scenario cannot exceed the latency-requirement $T_i^{\max}$. We emphasize that in (34), the auxiliary variables $\{\alpha_i\}_{i\in\mathcal{I}}$ and $\{\beta_{ik}\}_{i\in\mathcal{I},k\in\mathcal{K}}$ are not explicitly used as the decision variables, since they can be uniquely derived by all WDs' ordering $\boldsymbol{\pi}$ as well as each WD's $(t_i, \mathbf{s}_i)$. However, Problem (MultiWD) is much more complicated to solve than Problem (TECM) before, since it invokes a joint optimization of all WDs as well as the offloading ordering among them, which is a complicated combinatorial optimization problem. It is noticed that even with a given ordering $\boldsymbol{\pi}$, Problem (MultiWD) is still a strictly non-convex optimization problem.

6 Proposed Algorithm for Multi-WDs Scenario

6.1 Proposed Algorithm for the Multi-WDs Scenario

In spite of the strict non-convexity of Problem (MultiWD), we aim at proposing an efficient algorithm for solving it. The key of our design is to adopt a decomposition approach. Specifically, we first consider that the WDs' offloading-ordering $\boldsymbol{\pi}$ is given in advance, and exploit our Top-Algorithm as a subroutine for myopically minimizing each WD's energy consumption in sequence. Based on the obtained total energy consumption of all WDs, we then further optimize the WDs' ordering $\boldsymbol{\pi}$. The details of our decomposition can be illustrated as follows.

6.1.1 Myopically Optimizing Each WD's Energy Consumption Under a Given Ordering π

We first assume that the offloading ordering π is given in advance. Given π, we myopically minimize each WD's energy consumption one by one according to the ordering π. Specifically, given the time-instances of $(\alpha_{\pi(i)-1}, \{\beta_{\pi(i)-1,k}\}_{k\in\mathcal{K}})$ from the previous WD in ordering π, we individually minimize WD i's energy consumption by solving the following sub-problem:

$$\text{(MultiWD-Sub)}:$$

$$\hat{E}_{i,(\boldsymbol{\pi})} = \min \frac{S_i^{\text{req}} - \sum_{k\in\mathcal{K}} s_{ik}}{V_i^{\text{Loc}}} \rho_i^{\text{Loc}} + t_i \sum_{k\in\mathcal{K}} p_{ik}$$

$$\text{subject to: } 0 \le s_{ik} \le S_i^{\text{req}}, \forall k \in \mathcal{K}, \tag{35}$$

$$\sum_{k\in\mathcal{K}} s_{ik} \le S_i^{\text{req}}, \tag{36}$$

$$0 \leq \epsilon_i \leq \epsilon_i^{\max}, \tag{37}$$

$$\boldsymbol{\alpha}_{\pi(i)} = \boldsymbol{\alpha}_{\pi(i)-1} + t_i, \tag{38}$$

$$\boldsymbol{\beta}_{\pi(i),k} = \max\{\boldsymbol{\beta}_{\pi(i)-1,k}, \boldsymbol{\alpha}_{\pi(i)}\} + \frac{s_{ik}}{V_k}, \forall k \in \mathcal{K}, \tag{39}$$

$$\max\{\max_{k\in\mathcal{K}}\{\boldsymbol{\beta}_{\pi(i),k}\} - \boldsymbol{\alpha}_{\pi(i)-1}, \frac{S_i^{\mathrm{req}} - \sum_{k\in\mathcal{K}} s_{ik}}{V_i^{\mathrm{Loc}}}\} \leq T_i^{\max}, \tag{40}$$

$$\text{and constraints (4) and (5),}$$

$$\text{variables: } \mathbf{s}_i, t_i, \text{ and } \epsilon_i.$$

A key observation on Problem (MultiWD-Sub) is as follows. Since the values of $(\boldsymbol{\alpha}_{\pi(i)-1}, \{\boldsymbol{\beta}_{\pi(i)-1,k}\}_{k\in\mathcal{K}})$ are known when WD i executes its offloading-transmission, we can slightly modify our previously proposed Top-Algorithm by changing the values of $\{s_{ik}^{\mathrm{upp}}\}$ in the initial step in Sub-Algorithm and obtain the corresponding minimum energy consumption $\hat{E}_{i,(\boldsymbol{\pi})}$. We illustrate the detailed modifications in Section 6.2. Thus, by further using Top-Algorithm as a subroutine, we propose the following algorithm (i.e., MyoSeq-Algorithm) to minimize the total energy consumption of all WDs under a given $\boldsymbol{\pi}$.

MyoSeq-Algorithm To Minimize the Total Energy Consumption of All WDs in Sequence Under a Given Ordering $\boldsymbol{\pi}$

1: **Initialization:** Set $\hat{E}_{(\boldsymbol{\pi})}^{\mathrm{tot}} = 0$. Set $\boldsymbol{\alpha}_0 = 0$ and $\boldsymbol{\beta}_{0,k} = 0, \forall k \in \mathcal{K}$. Set flag $= 1$.
2: **while** Enumerating all WDs in sequence according to ordering $\boldsymbol{\pi}$ **do**
3: Let index $i \in \mathcal{I}$ to denote the WD currently being enumerated. Given $(\boldsymbol{\alpha}_{\pi(i)-1}, \{\boldsymbol{\beta}_{\pi(i)-1,k}\}_{k\in\mathcal{K}})$, use Top-Algorithm to obtain the corresponding $\hat{E}_{i,(\boldsymbol{\pi})}$ and the associated $\hat{t}_i$ and $\hat{\mathbf{s}}_i$. If Top-Algorithm outputs that Problem (MultiWD-Sub) is infeasible, set flag $= 0$ and go to Step 8 directly.
4: Update $\hat{E}_{(\boldsymbol{\pi})}^{\mathrm{tot}} = \hat{E}_{(\boldsymbol{\pi})}^{\mathrm{tot}} + \hat{E}_{i,(\boldsymbol{\pi})}$.
5: Update $\boldsymbol{\alpha}_{\pi(i)} = \boldsymbol{\alpha}_{\pi(i)-1} + \hat{t}_i$.
6: Update $\boldsymbol{\beta}_{\pi(i),k} = \max\{\boldsymbol{\beta}_{\pi(i)-1,k}, \boldsymbol{\alpha}_{\pi(i)}\} + \frac{\hat{s}_{ik}}{V_k}, \forall k \in \mathcal{K}$.
7: **end while**
8: **Output**: If flag $= 1$, output the total energy consumption $\hat{E}_{(\boldsymbol{\pi})}^{\mathrm{tot}}$ for all WDs. Otherwise, output the currently given ordering $\boldsymbol{\pi}$ is infeasible.

6.1.2 Top-Problem for Optimizing the Ordering $\boldsymbol{\pi}$

By using MyoSeq-Algorithm to obtain the total energy consumption of all WDs under a given offloading ordering $\boldsymbol{\pi}$, we then continue to optimize the ordering $\boldsymbol{\pi}$, with the objective of further minimizing all WDs' total energy consumption, i.e.,

$$\text{(MultiWD-Top):} \quad \min \hat{E}_{(\boldsymbol{\pi})}^{\mathrm{tot}}$$
$$\text{variable:} \quad \boldsymbol{\pi}.$$

Despite its simple form, Problem (MultiWD-Top) is extremely challenging to solve, since we cannot express $\hat{E}_{(\boldsymbol{\pi})}^{\mathrm{tot}}$ analytically. A straightforward manner is to enumerate all possible orderings of the WDs, which however, is computationally prohibitive when the number of the WDs is large. To address this difficulty, we propose a Swapping-Heuristic based algorithm (i.e., SH-Algorithm) to solve Problem (MultiWD-Top). Our SH-Algorithm works as follows.

- •: The key idea of our SH-Algorithm is to iteratively update the ordering $\boldsymbol{\pi}$ via swapping. Specifically, given the current ordering $\boldsymbol{\pi}$, we randomly select two WDs and swap their respective orders such that we obtain an updated ordering $\boldsymbol{\pi}^{\mathrm{udp}}$. If the updated ordering $\boldsymbol{\pi}^{\mathrm{udp}}$ can yield a smaller total energy consumption than the current ordering $\boldsymbol{\pi}$, we accept $\boldsymbol{\pi}^{\mathrm{udp}}$ for the next round of iteration.
- •: To avoid being trapped by some local optimum, we adopt the idea of annealing process [44]. Specifically, if the updated ordering $\boldsymbol{\pi}^{\mathrm{udp}}$ yields a degraded (i.e., larger) total energy consumption compared to the current ordering $\boldsymbol{\pi}$, we then choose to accept this degraded ordering $\boldsymbol{\pi}^{\mathrm{udp}}$ with a certain probability which depends on the gap between the two consecutive orderings as well as the current system temperature (i.e., from Step 9 to Step 15 in SH-Algorithm). Specifically, the likelihood for accepting a degraded ordering decreases, when T_l decreases. According to [45], the type of the cooling scheduling $T_l = \frac{T^{\mathrm{ini}}}{\ln(l)}$ can provide an asymptotic convergence to the global optimum solutio with a sufficiently large T^{ini}.

SH-Algorithm To Solve Problem (MultiWD-Top)

1: **Initialization:** Set the initial parameter T^{ini} as a large number, and the parameter for convergence T^{end} as a relative small number. Initialize the iteration index $l = 0$, $T_l = T^{\mathrm{ini}}$, a feasible ordering $\boldsymbol{\pi}_l$.
2: **while** $T_l \geq T^{\min}$ **do**
3: Given the ordering $\boldsymbol{\pi}_l$, use MyoSeq-Algorithm to obtain the corresponding minimum energy E_l.
4: Randomly select two WDs in $\boldsymbol{\pi}_l$ and swap their respective positions, which leads to an updated ordering $\boldsymbol{\pi}_l^{\mathrm{upd}}$.
5: Given the updated ordering $\boldsymbol{\pi}_l^{\mathrm{upd}}$, use MyoSeq-Algorithm to obtain the corresponding minimum energy E_l^{upd}.
6: **if** $E_l^{\mathrm{upd}} < E_l$ **then**
7: Update $\boldsymbol{\pi}_{l+1} = \boldsymbol{\pi}_l^{\mathrm{upd}}$.
8: **else**
9: Set $\Delta = E_l^{\mathrm{upd}} - E_l$.
10: Generate a random number v according to a uniform distribution within [0,1].
11: **if** $v \leq \exp\{-(\frac{\Delta}{T_l})\}$ **then**
12: Update $\boldsymbol{\pi}_{l+1} = \boldsymbol{\pi}_l^{\mathrm{upd}}$.
13: **else**
14: Update $\boldsymbol{\pi}_{l+1} = \boldsymbol{\pi}_l$.
15: **end if**
16: **end if**
17: Update $l = l + 1$, and $T_l = \frac{T_0}{\ln(l+1)}$.
18: **end while**
19: **Output**: the ordering of the WDs $\boldsymbol{\pi}^* = \boldsymbol{\pi}_l$.

6.2 An Illustration of Modifying Top-Algorithm for Solving Problem (MultiWD-Sub)

In this section, we provide the detailed descriptions about how to modify our previous Top-Algorithm for solving

Problem (MultiWD-Sub). Notice that in Problem (MultiWD-Sub), the values of $(\alpha_{\pi(i)-1}, \{\beta_{\pi(i)-1,k}\}_{k\in\mathcal{K}})$ (i.e., the time-instances of the WD which is prior to WD i in ordering $\boldsymbol{\pi}$) are all known in advance. Specifically, with (40), we can obtain the following constraint:

$$\beta_{\pi(i),k} \leq T_i^{\max} + \alpha_{\pi(i)-1}, \forall k.$$

Further with (29), we could obtain the following one:

$$\max\{\beta_{\pi(i)-1,k}, \alpha_{\pi(i)-1} + t_i\} + \frac{s_{ik}}{V_k} \leq T_i^{\max} + \alpha_{\pi(i)-1}, \forall k.$$

The above constraint leads to the following two ones:

$$s_{ik} \leq V_k(T_i^{\max} + \alpha_{\pi(i)-1} - \beta_{\pi(i)-1,k}), \forall k, \tag{41}$$

$$s_{ik} \leq V_k(T_i^{\max} - t_i), \forall k. \tag{42}$$

As a result, for Problem (MultiWD-Sub) with given $(\alpha_{\pi(i)-1}, \{\beta_{\pi(i)-1,k}\}_{k\in\mathcal{K}})$, we can obtain the upper bound for s_{ik} as follows:

$$s_{ik}^{\text{upp}} = \min\{S_i^{\text{req}}, V_k\Big(T_i^{\max} + \alpha_{\pi(i)-1} - \beta_{\pi(i)-1,k}\Big), V_k(T_i^{\max} - t_i), (1-\epsilon_i)t_i W_k \log_2\left(\frac{\hat{g}_{ik}}{\theta_{ik}}\right)\}, \forall k \in \mathcal{K}. \tag{43}$$

By replacing (13) with (43) in the initial step of our proposed Sub-Algorithm in Section 4.2, we can again use our Top-Algorithm proposed before for solving Problem (MultiWD-Sub). In particular, the complexity and convergence of using our Top-Algorithm to solve Problem (MultiWD-Sub) are same as those for solving Problem (TECM). The details can be referred to the discussions at the end of Section 4.2, and we do not repeat them here due to the limited space.

6.3 Numerical Results

In this subsection, we demonstrate the numerical results for our proposed SH-Algorithm (and its subroutine MyoSeq-Algorithm) for the multi-WDs scenario. Specifically, we set up the network scenario as we use in Section 4.3 before, where the ECSs are uniformly located on a circle of radius 500m. Meanwhile, the group of WDs are randomly located within a plane within the center at (0,0) and the radius of 200m. The channel power gain from each WD to the ECSs are generated according to the path-loss model aforementioned. The other parameter-settings for the WDs and ECSs are also similar to those in Section 4.3.

Fig. 10 demonstrates the convergence of our proposed SH-Algorithm under 3-WD, 5-WD, and 7-WD cases. For the sake of comparison, we also enumerate all the possible orderings of the WDs for each case and obtain the corresponding minimum energy consumptions denoted by the horizontal dash-lines in Fig. 10. The results in Fig. 10 show that our SH-Algorithm can efficiently converge to the best ordering of the WDs for Problem (MultiWD-Top) for all the tested cases.

Fig. 11 further shows the performance comparison between our SH-Algorithm and a heuristic randomized

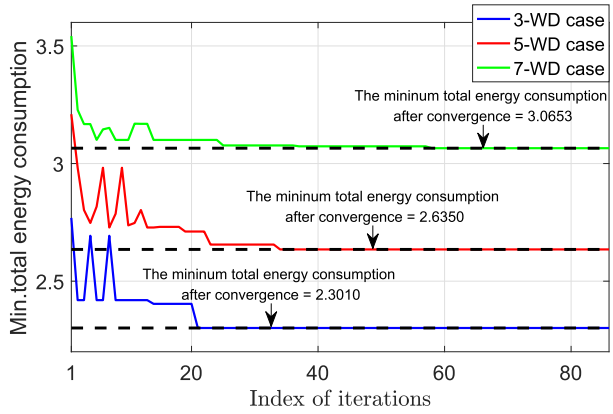

Fig. 10. Convergence of our SH-Algorithm under different cases.

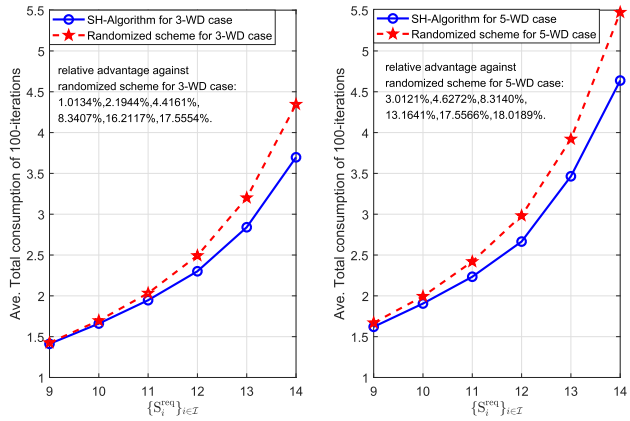

Fig. 11. Performance comparison between our proposed SH-Algorithm and the randomized WD-ordering scheme.

ordering scheme. Specifically, in the randomized ordering scheme, we randomly generate the ordering of the WDs for executing the multi-access offloading, and each point of the randomized ordering scheme in Fig. 11 denotes the average result of the 100 randomly generated orderings of the WDs. It is worth emphasizing that although the WDs are randomly ordered in the randomized WD-ordering scheme, we still optimize each individual WD's multi-access offloading decision, secrecy-provisioning, and the transmission-duration, with the objective of minimizing its total energy consumption (i.e., solving Problem (MultiWD-Sub) to obtain each WD i's optimal multi-offloading solution under the given time-instances $(\alpha_{(\pi(i))-1}, \{\beta_{\pi(i)} - 1\}_{k\in\mathcal{K}})$ of the WD who executes the offloading just prior to WD i). Therefore, the considered randomized WD-ordering scheme can provide a meaningful benchmark for evaluating the performance of our proposed SH-Algorithm. Specifically, the left-subplot shows the results for a 3-WD case, and the right-subplot shows the results for a 5-WD case. The results in both cases demonstrate that our SH-Algorithm can outperform the randomized ordering scheme. Moreover, as denoted by the line of the number in each subplot, the relative advantages of our SH-Algorithm against the randomized ordering scheme gradually increase when the WDs' computation-workload requirements increase, which means that the proper ordering of the WDs in executing the multi-access offloading will play a more significant role when the WDs' computation-workload requirements become larger.

7 Conclusion

In this work, we have studied the energy-efficient multi-access MEC with secrecy provisioning. For the single-WD scenario, we have formulated a joint optimization of the WD's multi-access computation offloading, secrecy provisioning, and offloading-transmission duration, with the objective of minimizing the WD's total energy consumption in completing its workload, while providing a guaranteed secrecy-provisioning as well as a guaranteed overall-latency in completing the required workload. Despite the non-convexity of this joint optimization problem, we have exploited its layered structure and proposed an efficient algorithm for solving it. Exploiting our study on single-WD scenario as a basis, we further investigated the multi-WDs scenario subject to a malicious node's eavesdropping. Taking the coupling effect among different WDs into account, we have proposed an efficient algorithm for finding the ordering of WDs in executing multi-access computation offloading, with the objective of minimizing all WDs' total energy consumption. Extensive numerical results have been provided to validate the effectiveness and efficiency of our proposed algorithms. The results have demonstrated that the advantages of our algorithms in saving the energy consumption while providing a guaranteed secrecy and a guaranteed latency in completing the tasks. In our future work, we will investigate a multi-WDs scenario in which different WDs use orthogonal frequency division multiple access for enabling their respective multi-access offloading transmissions simultaneously. In addition, it is also important for us to further investigate the multi-antenna scenario in which the BS (or the eavesdropper) is equipped with multiple antennas for enhancing the data reception (or the overhearing capability).

Acknowledgments

This work was supported in part by the National Natural Science Foundation of China under Grants 62071431 and 62072490, in part by Science and Technology Development Fund of Macau SAR under Grants 0060/2019/A1 and 0162/2019/A3, in part by FDCT-MOST Joint Project under Grant 0066/2019/AMJ, in part by the Intergovernmental International Cooperation in Science and Technology Innovation Program under Grants 2019YFE0111600, and in part by Research Grant of University of Macau under Grants MYRG2018-00237-FST and SRG2019-00168-IOTSC. The work of Dr. Weijia Jia was supported by the Guangdong Key Lab of AI and Multi-modal Data Processing, National Natural Science Foundation of China under Grant 61872239, and BNU-UIC Institute of Artificial Intelligence and Future Networks funded by Beijing Normal University (Zhuhai) and AI-DS Research Hub, BNU-HKBU United International College (UIC), Zhuhai, China.

References

[1] S. Kekki *et al*. "MEC in 5G networks," Sophia Antipolis, France, ETSI White Paper no. 28, Jun. 2018.

[2] C. Wang, Y. He, F. R. Yu, Q. Chen, and L. Tang, "Integration of networking, caching, and computing in wireless systems: A survey, some research issues, and challenges," *IEEE Commun. Surv. Tut.*, vol. 20, no. 1, pp. 7–38, First Quarter 2018.

[3] N. Abbas, Y. Zhang, A. Taherkordi, and T. Skeie, "Mobile edge computing: A survey," *IEEE Internet Things J.*, vol. 5, no. 1, pp. 450–465, Feb. 2018.

[4] Y. Mao, C. You, J. Zhang, K. Huang, and K. B. Letaief, "A survey on mobile edge computing: The communication perspective," *IEEE Commun. Surv. Tut.*, vol. 19, no. 4, pp. 2322–2358, Fourth Quarter 2017.

[5] Q.-V. Pham, *et al*. "A survey of multi-access edge computing in 5G and beyond: Fundamentals, technology integration, and state-of-the-art," *IEEE Access*, vol. 8, pp. 116974–117017, Jan. 2020.

[6] T. Taleb, K. Samdanis, B. Mada, H. Flinck, S. Dutta, and D. Sabella, "On multi-access edge computing: A survey of the emerging 5G network edge cloud architecture and orchestration," *IEEE Commun. Surv. Tut.*, vol. 19, no. 3, pp. 1657–1681, Third Quarter 2017.

[7] H. Guo, J. Liu, and J. Zhang, "Computation offloading for multi-access mobile edge computing in ultra-dense networks," *IEEE Commun. Mag.*, vol. 56, no. 8, pp. 14–19, Aug. 2018.

[8] L. Li, T. Q. S. Quek, J. Ren, H. H. Yang, Z, Chen, and Y. Zhang, "An incentive-aware job offloading control framework for multi-access edge computing," *IEEE Trans. Mobile Comput.*, vol. 20, no. 1, pp. 63–75, Jan. 2021.

[9] H. A. Alameddine, S. Sharafeddine, S. Sebbah, S. Ayoubi, and C. Assi, "Dynamic task offloading and scheduling for low-latency IoT services in multi-access edge computing," *IEEE J. Sel. Areas Commun.*, vol. 37, no. 3, pp. 668–682, Mar. 2019.

[10] X. Chen, H. Zhang, C. Wu, S. Mao, Y. Ji, and M. Bennis, "Optimized computation offloading performance in virtual edge computing systems via deep reinforcement learning", *IEEE Internet Things J.*, vol. 6, no. 3, pp. 4005–4018, Jun. 2019.

[11] R. Deng, R. Lu, C. Lai, T. H. Luan, and H. Liang, "Optimal workload allocation in fog-cloud computing toward balanced delay and power consumption," *IEEE Internet Things J.*, vol. 3, no. 6, pp. 1171–1181, Dec. 2016.

[12] Q.-V. Pham, H.T. Nguyen, Z. Han, W.-J. Hwang, "Coalitional games for computation offloading in NOMA-enabled multi-access edge computing," *IEEE Trans. Veh. Technol.*, vol. 69, no. 2, pp. 1982–1993, Feb. 2020.

[13] Y. Zhang, D. Niyato, and P. Wang, "Offloading in mobile cloudlet systems with intermittent connectivity," *IEEE Trans. Mobile Comput.*, vol. 14, no. 12, pp. 2516–2529, Dec. 2015.

[14] L. Liu, Z. Chang, X. Guo, S. Mao, and T. Ristaniemi, "Multi-objective optimization for computation offloading in fog computing," *IEEE Internet Things J.*, vol. 5, no. 1, pp. 283–294, Feb. 2018.

[15] T. Q. Dinh, Q. D. La, T. Q. Quek, and H. Shin, "Learning for computation offloading in mobile edge computing," *IEEE Trans. Commun.*, vol. 66, no. 12, pp. 6353–6367, Aug. 2018.

[16] Z. Chang, W. Guo, X. Guo, Z. Zhou, and T. Ristaniemi, "Incentive mechanism for edge computing-based blockchain," *IEEE Trans. Ind. Inform.* vol. 16, no. 11, pp. 7105–7114, Nov. 2020.

[17] Z. Kuang, L. Li, J. Gao, L. Zhao, and A. Liu, "Partial offloading scheduling and power allocation for mobile edge computing systems," *IEEE Internet Things J.*, vol. 6, no. 4, pp. 6774–6785, Aug. 2019.

[18] Y. Wu, K. Ni, C. Zhang, L. Qian, and D. H. K. Tsang, "NOMA assisted multi-access mobile edge computing: A joint optimization of computation offloading and time allocation," *IEEE Trans. Veh. Technol.*, vol. 67, no. 12, pp. 12244–12258, Dec. 2018.

[19] L. Huang, S. Bi, and Y.J. Zhang, "Deep reinforcement learning for online computation offloading in wireless powered mobile-edge computing networks," *IEEE Trans. Mobile Comput.*, vol. 19, no. 11, pp. 2581–2593, Nov. 2020.

[20] M. Sheng, Y. Dai, J. Liu, N. Cheng, X. Shen, and Q. Yang, "Delay-aware computation offloading in NOMA MEC under differentiated uploading delay," *IEEE Trans. Wirel. Commun.*, vol. 19, no. 4, pp. 2813–2826, Apr. 2020.

[21] H. Peng, Q. Ye, and X. Shen, "Spectrum management for multi-access edge computing in autonomous vehicular networks," *IEEE Trans. Intell. Transp. Syst.*, vol. 21, no, 7, pp. 3001–3012, Jul. 2019.

[22] Y. Gu, Z. Chang, M. Pan, L. Song, and Z. Han, "Joint RADIO AND COMPUTATIONAL RESOURCE ALLOCAtion in IoT fog computing," *IEEE Trans. Veh. Technol*, vol. 67, no. 8, pp. 7475–7484, Aug. 2018.

[23] J. Feng, F.R. Yu, Q. Pei, J. Du, and L. Zhu, "Joint optimization of radio and computational resources allocation in blockchain-enabled mobile edge computing systems," *IEEE Trans. Wirel. Commun.*, vol. 19, no. 6, pp. 4321–4334, Jun. 2020.

[24] Z. Zhou, J. Feng, Z. Chang, and X. Shen, "Energy-efficient edge computing service provisioning for vehicular networks: A consensus ADMM approach," *IEEE Trans. Veh. Technol.*, vol. 68, no. 5, pp. 5087–5099, May 2019.
[25] Z. Chang, Z. Zhou, T. Ristaniemi, and Z. Niu, "Energy efficient optimization for computation offloading in fog computing system," in *Proc. IEEE Global Commun. Conf.*, 2017, pp. 1–6
[26] M. Li, N. Chen, Y. Wang, J. Gao, L. Zhao, and X. Shen, "Energy-efficient UAV-assisted mobile edge computing: Resource allocation and trajectory optimization," *IEEE Trans. Veh. Technol.*, vol. 69, no. 3, pp. 3424–3438, Mar. 2020.
[27] E. Haber, T.M. Nguyen, and C. Assi, "Joint optimization of computational cost and devices energy for task offloading in multi-tier edge-clouds," *IEEE Trans. Commun.*, vol. 67, no. 5, pp. 3407–3421, May 2019.
[28] Y. Wu, B. Shi, L. Qian, F. Hou, J. Cai, and X. Shen, "Energy-efficient multi-task multi-access computation offloading via NOMA transmission for IoTs," *IEEE Trans. Ind. Inform.*, vol. 16, no. 7, pp. 4811–4822, Jul. 2020.
[29] K. Zhang, *et al.*, "Energy-efficient offloading for mobile edge computing in 5G heterogeneous networks," *IEEE Access*, vol. 4, pp. 5896–5907, Aug. 2016.
[30] M. Min, L. Xiao, Y. Chen, P. Cheng, D. Wu, and W. Zhuang, "Learning-based computation offloading for IoT devices with energy harvesting," *IEEE Trans. Veh. Technol.*, vol. 68. no. 2, pp. 1930–1941, Feb. 2019.
[31] S. Bi and Y. J. A. Zhang, "Computation rate maximization for wireless powered mobile-edge computing with binary computation offloading," *IEEE Trans. Wirel. Commun.*, vol. 17, no. 6, pp. 4177–4190, Jun. 2018.
[32] F. Wang, J. Xu, X. Wang, and S. Cui, "Joint offloading and computing optimization in wireless powered mobile-edge computing systems," *IEEE Trans. Wirel. Commun.*, vol. 17, no. 3, pp. 1784–1797, Mar. 2018.
[33] A. D. Wyner, "The wire-tap channel," *Bell Syst. Tech. J.*, vol. 54, no. 8, pp. 1355–1387, Oct. 1975.
[34] A. Mukherjee, S. A. A. Fakoorian, J. Huang and A. L. Swindlehurst,, "Principles of physical layer security in multiuser wireless networks: A survey," *IEEE Commun. Surveys Tut.*, vol. 16, no. 3, pp. 1550–1573, Third Quarter 2014.
[35] Y. Wu, K. Guo, J. Huang, and X. Shen, "Secrecy-based energy-efficient data offloading via dual-connectivity over unlicensed spectrums," *IEEE J. Sel. Areas Commun.*, vol. 34, no. 12, pp. 3252–3270, Dec. 2016.
[36] Z. Chang, *et al.*, "Secure and energy-efficient resource allocation for multiple-antenna noma with wireless power transfer," *IEEE Trans. Green Commun. Netw.*, vol. 2, no. 4, pp. 1059–1071, Dec. 2018.
[37] Y. Sun, D. W. K. Ng, J. Zhu, and R. Schober, "Robust and secure resource allocation for full-duplex MISO multicarrier NOMA systems," *IEEE Trans. Commun.*, vol. 66, no. 9, pp. 4119–4137, Sep. 2018.
[38] L. Xiao, G. Sheng, S. Liu, H. Dai, M. Peng, and J. Song, "Deep reinforcement learning-enabled secure visible light communication against eavesdropping," *IEEE Trans. Commun.*, vol. 67, no. 10, pp. 6994–7005, Jul. 2019.
[39] D. Wang, B. Bai, K. Lei, W. Zhao, Y. Yang, and Z. Han, "Enhancing information security via physical layer approaches in heterogeneous IoT with multiple access mobile edge computing in smart city," *IEEE Access*, vol. 7, pp. 54508–54521, May 2019.
[40] J. Xu and J. Yao, "Exploiting physical-layer security for multiuser multicarrier computation offloading," *IEEE Wirel. Commun. Lett.*, vol. 8, no. 1, pp. 9–12, Feb. 2019.
[41] Y. Wu, *et al.*, "Secrecy-driven resource management for vehicular computation-offloading networks," *IEEE Netw.*, vol. 32, no. 3, pp. 84–91, Jun. 2018.
[42] W. Wu, F. Zhou, R. Q. Hu, and B. Wang, "Energy-efficient resource allocation for secure NOMA-enabled mobile edge computing networks," *IEEE Trans. Commun.*, vol. 68, no. 1, pp. 493–505, Jan. 2020.
[43] L. Schrage, *Optimization Modeling with LING O. Chicago*, IL, USA: Lindo System, 1999.
[44] D. Bertsimas and J. Tsitsiklis, "Simulated annealing," *Stat. Sci.*, vol. 8, no. 1, pp. 10–15, 1993.
[45] J. F. Martin and J. M. Sierra, "A comparison of cooling schedules for simulated annealing," in *Encyclopedia of Artificial Intelligence*, Hershey, PA, USA: Inf. Sci. Ref., 2009, ch. 53, pp. 344–352.

Li Ping Qian (Senior Member, IEEE) received the Ph.D. degree in information engineering from the Chinese University of Hong Kong in 2010. From 2010 to 2011, she was a postdoctoral research associate with The Chinese University of Hong Kong. Since 2011, she has been with the College of Information Engineering, Zhejiang University of Technology, Hangzhou, China, where she is currently a full professor. From 2016 to 2017, she was a visiting scholar with the Broadband Communications Research Group, ECE Department, University of Waterloo. Her research interests include wireless communication and networking, resource management in wireless networks, massive IoTs, mobile edge computing, emerging multiple access techniques, and machine learning oriented toward wireless communications. She is currently on the Editorial Board of IET *Communications*. She was the corecipient of the IEEE Marconi Prize Paper Award in *IEEE Wireless Communications* in 2011, the Best Paper Award from IEEE ICC 2016, and the Best Paper Award from IEEE Communication Society GCCTC 2017.

Yuan Wu (Senior Member, IEEE) received the Ph.D. degree in electronic and computer engineering from the Hong Kong University of Science and Technology in 2010. He is currently an associate professor with the State Key Laboratory of Internet of Things for Smart City, University of Macau, and also with the Department of Computer and Information Science, University of Macau. He was a full professor with the College of Information Engineering, Zhejiang University of Technology, Hangzhou, China. From 2016 to 2017, he was a visiting scholar with Department of Electrical and Computer Engineering, University of Waterloo. His research interests include resource management for wireless networks, green communications and computing, mobile edge computing, and smart grids. He was the guest editors of *IEEE Communications Magazine*, *IEEE Network*, *IEEE Transactions on Industrial Informatics*, and *IET Communications*. He is currently on the Editorial Boards of the *IEEE Internet of Things Journal*, *IEEE Open Journal of the Communications Society*, *and China Communications*. He was the recipient of the Best Paper Award from the IEEE International Conference on Communications in 2016 and the Best Paper Award from the IEEE Technical Committee on Green Communications and Computing in 2017.

Ningning Yu is currently working toward the M.S. degree from the College of Information Engineering, Zhejiang University of Technology, Hangzhou, China. His research interests include artificial intelligence and deep learning, with their applications in wireless networks and mobile edge computing.

Daohang Wang is currently working toward the M.S. degree from the College of Information Engineering, Zhejiang University of Technology, Hangzhou, China. His research interests include physical layer security in wireless networks and mobile edge computing.

Fuli Jiang received the M.S. degree from the University of Electronic Science and Technology of China in 2017. He was a research assistant with the State Key Laboratory of Internet of Things for Smart City, University of Macau, Macao, China. He is currently a research assistant with The Chinese University of Hong Kong, Hong Kong. His research interests include resource management for mobile edge computing and Internet of Things.

Weijia Jia (Fellow, IEEE) received the B.Sc. and M.Sc. degrees in computer science from Center South University, China, in 1982 and 1984, respectively, and the master of applied science and Ph.D. degrees in computer science from the Polytechnic Faculty of Mons, Belgium, in 1992 and 1993, respectively. He is currently the chair-professor and director of BNU-UIC Institute of Artificial Intelligence and Future Networks, Beijing Normal University (Zhuhai), China. He was the chair professor and deputy director with the State Kay Laboratory of Internet of Things for Smart City, the University of Macau. He was the Zhiyuan chair professor with Shanghai Jiaotong University, China. From 1993 to 1995, he joined German National Research Center for Information Science (GMD), Bonn (St. Augustine), as a research fellow. From 1995 to 2013, he was a professor with the City University of Hong Kong. He has authored or coauthored more than 500 papers in the prestige international journals or conferences and research books and book chapters. His contributions have been recognized as optimal network routing and deployment, vertex cover, anycast and QoS routing, sensors networking, knowledge relation extractions, NLP, and edge computing. He was an area editor for various prestige international journals, chair and PC member or keynote speaker for many top international conferences. He is currently a distinguished member of Congestive Cardiac Failure. He was the recipient of the Best Product Awards from the International Science and Tech. Expo, Shenzhen, in 2011–2012 and the first Prize of Scientific Research Awards from the Ministry of Education of China in 2017 (list 2).